Meso-Cenozoic morphotectonic evolution of southern Norway: Neogene domal uplift inferred from apatite fission track thermochronology

Rohrmann, M.; van der Beek, P.A.; Andriessen, P.; Cloetingh, S.A.P.L.

published in
Tectonics
1995

DOI (link to publisher)
10.1029/95TC00088

document version
Publisher's PDF, also known as Version of record

TECTONICS, VOL. 14, NO. 3, PAGES 704-718 , JUNE 1995

Meso-Cenozoic morphotectonic evolution of southern Norway: Neogene domal uplift inferred from apatite fission track thermochronology

Max Rohrman, Peter van der Beek, Paul Andriessen, and Sierd Cloetingh

Faculty of Earth Sciences, Vrije Universiteit, Amsterdam, Netherlands

Abstract. Apatite fission track (AFT) thermochronology of Precambrian and Paleozoic basement samples from southern Norway reveals a post-Paleozoic exhumation history, related to offshore Mesozoic and Cenozoic extensional basin development. The data indicate two major phases of rapid exhumation. A first Mesozoic phase started in the Triassic (~220 Ma) in the east and south of the study area and migrated to the west where Jurassic (~160 Ma) ages of exhumation predominate. A second event is indicated by thermal history modeling of AFT ages and track length distributions. It is inferred to be Neogene in age, initiated at about 30 Ma, and it produced a domal pattern of AFT isochrons which follow present-day topographic elevation. Youngest AFT ages (~100 Ma) are encountered at sealevel in the inner fjords near the areas of highest topography; ages increase radially outward to the mountain peaks and the coastlines. Forward modeling of age-elevation patterns suggests that Mesozoic geothermal gradients were 10-15°C/km higher than the present value of 20°C/km. During the Triassic and Jurassic, a total of 1.3-3.5 km of overburden was removed from the study area, assuming a 30°C/km geothermal gradient for that period. We attribute this to rift margin erosion as a result of erosional base level lowering and flank uplift, as evidenced by thick continental clastic sequences deposited in Triassic-Jurassic half grabens in the North Sea basins. We propose that 1.5-2.5 km of Neogene exhumation were a result of late stage domal uplift. This is supported by basinward dipping pre-Neogene strata in the basins surrounding southern Norway and the infill of a 1- to 2-km-thick Neogene sediment wedge containing various internal unconformities. Domal uplift probably started in the Late Oligocene, may have been amplified in the Pliocene, and was overprinted by Plio-Pleistocene glacial erosion. Maximum Neogene tectonic uplift is estimated at approximately 1-1.5 km, radially decreasing outward to a value <500 m near the shoreline. Neogene domal uplift is coincident with Oligocene and Pliocene plate reorganizations in the North Atlantic; similar Neogene domes are found around the Norwegian-Greenland Sea (i.e., Svalbard and the Barents Sea, northern Norway, east Greenland), suggesting a regional tectonic cause. The onset of Neogene uplift postdates major volcanism and continental breakup by ~25 m.y. and predates Plio-Pleistocene glaciations. Its origin is possibly a combination of induced mantle convection, resulting in thermal erosion of the lithosphere, and the operation of intraplate stresses.

Paper number 95TC00088.
0278-7407/95/95TC-00088$10.00

Introduction

It has become apparent in recent years that rifted margins may record significant postrift (late stage) uplift events, in addition to better understood synrift flank uplift [e.g., *Cloetingh and Kooi,* 1992; *Sales,* 1992]. For instance, *Cloetingh et al.* [1990; 1992] stress the importance of accelerated postrift subsidence, in conjunction with margin uplift, for various basins on both sides of the North Atlantic during the Neogene.

The geomorphology of Norway and the almost complete absence of post-Paleozoic sediments have led geoscientists for decades to suggest large-scale Tertiary uplift of western Fennoscandia [e.g., *Holtedahl,* 1953; *Torske,* 1972]. The rugged morphology of the Paleozoic Caledonide orogen, the preservation of planation surfaces at high altitudes [*Gjessing,* 1967; *Peulvast,* 1985] (Figure 1) and the absence of a crustal root under the orogen [*Theilen and Meissner,* 1979; *Andersen et al.,* 1991], suggest that the morphotectonic evolution of Norway was strongly affected by Meso-Cenozoic tectonic and climatic events in the North Sea and North Atlantic regions, rather than being solely the result of Caledonian orogeny. However, the exact timing and mechanism of uplift and erosion, as well as the influence of Quaternary glaciations, remain a matter of controversy.

Over the last 20 years, knowledge of the tectonic and paleogeographic evolution of the Norwegian offshore sedimentary basins has increased dramatically as a result of intense hydrocarbon exploration [cf. *Ziegler,* 1990; *Doré,* 1991]. The basins record substantial late Cenozoic uplift and erosion of the Norwegian mainland, evidenced by a structural basinward dip of the pre-Neogene strata and the buildup of large clastic wedges [*Stuevold et al.,* 1992; *Jensen and Schmidt,* 1993]. In contrast to the margins, the onshore Meso-Cenozoic evolution remains largely unresolved, due to the lack of sediments.

In the absence of a sedimentary record, apatite fission track (AFT) thermochronology provides practically the only means to resolve vertical motions of the order of a few kilometers within the upper crust. AFT age-elevation and age-length trends provide tight constraints on the amount and timing of exhumation [e.g., *Gleadow and Fitzgerald,* 1987; *Omar et al.,* 1989]. Recent advances in the understanding of AFT annealing kinetics [*Laslett et al.,* 1987; *Crowley et al.,* 1991] now allow the quantification of low-temperature

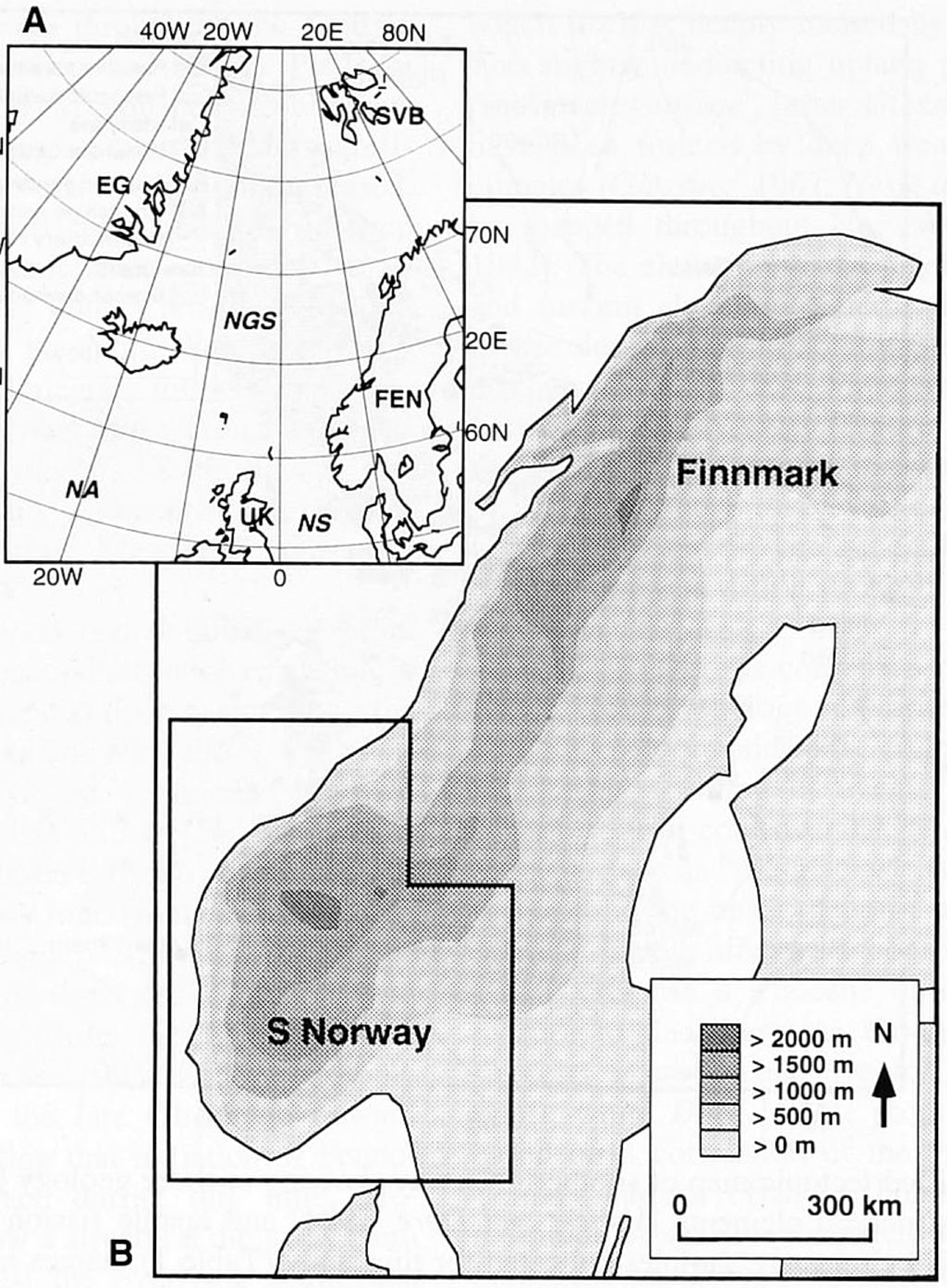

Figure 1. (a) Regional map of the North Atlantic. Notations are FEN Fennoscandia; NGS Norwegian-Greenland Sea; EG east Greenland; SVB Svalbard; UK United Kingdom; NS North Sea; NA North Atlantic. (b) Elevation of "paleic surface" in western Fennoscandia (modified from *Gjessing,* 1967). Inset shows extent of study area (Figure 2).

(<120°C) cooling and exhumation paths [*Green et al.,* 1989; *Lutz and Omar,* 1991]. Mapping regional variations in AFT ages and confined track lengths has proven to be a powerful approach in unraveling the history and style of exhumation of areas devoid of sediments [e.g., *Brown et al.,* 1994].

In this paper, we report on a regional AFT thermochronology study in southern Norway. We present new data and integrate the results of earlier studies [*Van den haute,* 1977; *Andriessen and Bos,* 1986; *Andriessen,* 1990; *Stiberg,* 1993; *Grønlie et al.,* 1994] which focused on more local areas. Using this approach, we have mapped AFT data over a large region, extending over nearly 500 km from the Skagerrak in the southeast to the Møre-Trøndelag area in the northwest (Figure 2). We aim to constrain the vertical movements of the southern Norwegian mainland and study the relation between Neogene basin subsidence and margin evolution. We compare our results with geomorphological studies and offshore seismic-stratigraphic data, which we first briefly review, to arrive at an exhumation history from Triassic to recent times and estimates of the amount of associated tectonic uplift [*Brown,* 1991; *van der Beek et al.,* 1994]. The results of this study provide insights into the paleogeographic evolution of western Fennoscandia, the processes driving late stage vertical motions, and the timing of exhumation with respect to climatic change [e.g., *Molnar and England,* 1990].

Tectonic and Paleographic Evolution of southern Norway

Onshore Record: Precambrian-Paleozoic Orogenies

The onshore geology of southern Norway is dominated by Precambrian basement rocks of the Baltic Shield, which are overthrust from the northwest by the crystalline and sedimentary nappes of the Caledonides. In the southeast the basement is intersected by the NS trending Permo-Carboniferous Oslo Rift (Figure 2). The southwestern segment of the Baltic Shield, exposed in southern Norway, was accreted and partially reworked during the Gothian (1.75-1.5 Ga) and Sveconorwegian/Grenvillian (1.25-0.9 Ga) orogenies [*Verschure,* 1985; *Starmer,* 1993]. The Sveconorwegian orogeny terminated with the intrusion of post-orogenic granites at ~900 Ma and final uplift and denudation, followed by the opening of the Iapetus Ocean during the latest Vendian- earliest Cambrian (~650 Ma).

Subduction of oceanic crust led to closing of the Iapetus Ocean at ~400 Ma and suturing of the Baltic and Laurentian

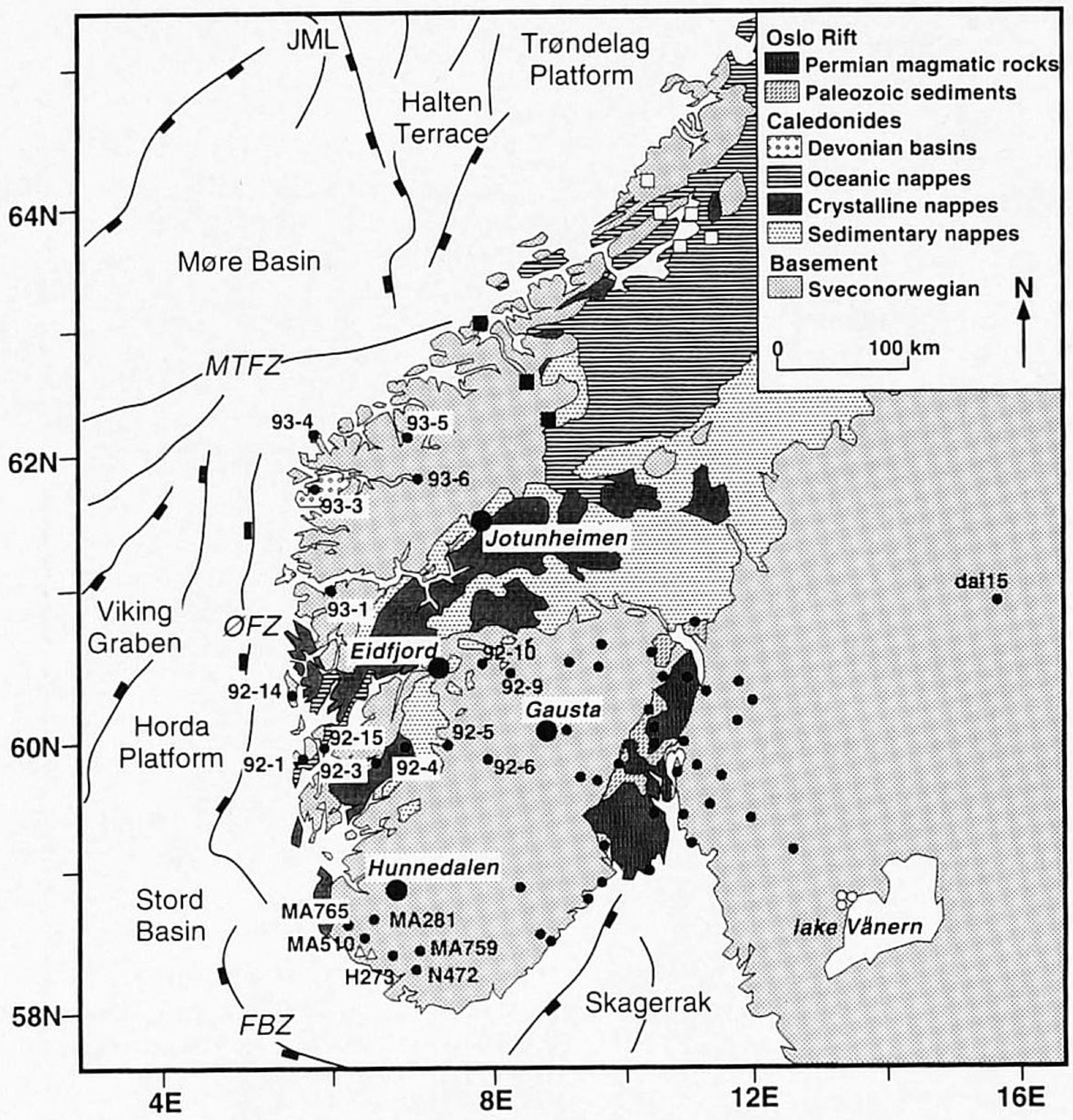

Figure 2. Simplified tectonic map of southern Norway showing onshore geology [after *Roberts and Gee,* 1985], offshore structural elements [*Vollset and Doré,* 1984] and apatite fission track (AFT) database. Labeled small solid circles are samples collected for this study (Table 1); names in italics and large solid circles give locations of elevation profiles. Unlabelled small solid circles are samples from *Rohrman et al.* [1994]; open circles are samples from *Zeck et al.* [1988]; filled squares are samples from *Stiberg* [1993]; open squares are samples from *Grønlie et al.* [1994]; open triangles are samples from *Van den haute* [1977]. Other notations are FBZ Fennoscandian Border Zone; JML Jan Mayen Lineament; MTFZ Møre-Trøndelag Fault Zone; ØFZ Øygarden Fault Zone.

plates during the Caledonian orogeny. The Caledonides represent a major continental collision belt, exposing obducted oceanic fragments, exhumed eclogitic rocks and reworked Baltic basement [e.g., *Roberts and Gee,* 1985; *Hossack and Cooper,* 1986]. Postorogenic collapse resulted in removal of the crustal root, asymmetric extension, and the development of fault-bounded Devonian molasse basins exposed around the Norwegian-Greenland Sea [*Andersen et al.,* 1991]. The Caledonian structural elements strongly influenced the position and development of later Mesozoic extensional basins in the North Sea and North Atlantic [*Doré,* 1991].

In the late Carboniferous, regional E-W extension, possibly related to Variscan orogenic activity toward the south [*Ziegler,* 1990] caused the formation of the highly magmatic Oslo Rift in southeastern Norway [*Neumann et al.,* 1992] and precursors of the Central and Viking grabens in the North Sea area. The onshore geological record ceases at the end of the Permian, leaving little trace of the post-Permian evolution.

Offshore Record: Meso-Cenozoic Basin Development

The offshore sedimentary record in the northern North Sea and Norwegian-Greenland Sea, as presently sampled by seismic and well data, dates back to the Permian. A phase of Permian-Early Triassic rifting is evidenced by thick Permo-Triassic clastic sequences, deposited in half grabens underlying the Viking Graben and Horda Platform [e.g., *Gabrielsen et al.,* 1990]. Major faulting activity, especially along the Øygarden Fault Zone, dates back to this time (Figure 2). Permo-Triassic sedimentation was almost entirely continental, except for a Late Permian transgression leading to the deposition of a thick evaporite sequence (Zechstein salts) in the south and carbonates in the north [*Ziegler,* 1990; *Doré,* 1991]. A second transgression took place in the Early Jurassic, possibly as a result of ongoing or renewed extension. This was followed in the Middle Jurassic (Toarcian-Bathonian) by major uplift in the central North Sea [*Ziegler,* 1990], accompanied by extensive alkaline volcanism. This event led to the development of large deltaic systems throughout the northern North Sea which are now the main target of hydrocarbon exploration. The North Sea dome collapsed in the Late Jurassic (Oxfordian-Volgian), giving way to the final and major phase of rifting in the Viking Graben. Mesozoic extensional episodes are also recorded by Permian to Middle Jurassic alkaline dikes cropping out on the islands of western Norway [*Færseth et al.,* 1976]. The buildup of coarse clastic sequences throughout the Triassic and Jurassic in the Viking Graben and Horda Platform [*Gabrielsen et al.*, 1990; *Steel*, 1993] indicates a continuous supply of clastics from the Norwegian mainland and significant erosion. During the Cretaceous the influx decreased, which, together with rapid postrift subsidence, led to deep starved basins and extensive organic shale sedimentation. A major transgression during the Late Cretaceous caused widespread chalk deposition in the North Sea area. Early Jurassic and Late Cretaceous sedimentary inliers which have been discovered onshore, along the Møre-Trøndelag Fault Zone in mid-Norway [*Bøe and Bjerkli*, 1989], indicate that the edges of the basin substantially overstepped the present-day coastline of Norway during Mesozoic highstands [*Ziegler*, 1990; *Doré*, 1991].

While the North Sea developed into a failed rift basin after Late Jurassic times, Cretaceous-Paleocene extension in the Norwegian-Greenland Sea created deep basins along the Vøring and Møre margins [*Brekke and Riis*, 1987], culminating in major volcanic activity and continental breakup between Norway and Greenland at 55 Ma [*Skogseid et al.*, 1992]. During the Paleogene, clastic influx from the Norwegian mainland was minor and only found in the Northwestern part of Southern Norway [*Rundberg and Smalley*, 1989]; the North Sea was dominated by deep water sedimentation, with most sediment supply coming from the Shetlands and Scottish highlands [*Galloway et al.*, 1993]. Sediment supply from Norway increased from the late Oligocene onward [*Stuevold et al.*, 1992], suggesting that initiation of Fennoscandian exhumation took place during this time. Pre-Neogene sedimentary strata show a structural dip away from the coastline and toplap against the overlying sediments, suggesting uplift of the mainland [*Doré*, 1992; *Jensen and Schmidt*, 1993]. Although the Øygarden and Møre-Trøndelag Fault Zones continue to display some seismic activity [*Gabrielsen*, 1989], seismic data do not record major post-Cretaceous vertical motions across these faults. Neogene uplift and Plio-Pleistocene glaciations resulted in extensive erosion and redeposition onshore and offshore, leading to a thick Neogene sedimentary wedge. The base of the Neogene wedge is dated at 33 Ma [*Rundberg and Smalley*, 1989]; it contains several unconformities and becomes sandier and more dominated by a Fennoscandian source upward [*Galloway et al.*, 1993]. Pliocene and younger ($\leq$5 Ma) deposits comprise approximately half the volume of the wedge [*Rundberg and Smalley*, 1989; *Ghazi*, 1992], suggesting an increase in erosion rates since then. A major unconformity occurs at ~2 Ma; this is interpreted as recording the onset of glacial erosion and redeposition [*Rundberg and Smalley*, 1989]. *Jansen and Sjøholm* [1991] infer an age of 2.57 Ma for the onset of major ice sheet expansion, based on dating of ice- rafted detritus; smaller-scale glaciations may have occurred from 5.45 Ma onward. The Neogene wedge can be traced all around the coast of southern and western Norway. A similar pattern of Neogene erosion and redeposition is encountered in the southwestern Barents Sea [*Doré*, 1991; *Riis and Fjeldskaar*, 1992].

Morphotectonic Evolution

The morphology of southern Norway is characterized by high mountain peaks rising above an elevated upland plateau which itself is deeply incised by narrow valleys and fjords. The slightly undulating upland plateau is generally termed the "paleic surface" [after *Gjessing*, 1967]. It is thought to have been formed by deep weathering in relatively warm climates [*Gjessing*, 1967; *Nesje and Whillans*, 1994] and can be mapped throughout Norway [cf. *Riis and Fjeldskaar*, 1992]. The elevation of the paleic surface follows the mean and summit elevation patterns, forming two distinct asymmetric domes, one in southwestern Norway and another in northern Sweden and Finnmark, with a low saddle in between in mid-Norway (Figure 1). In southwestern Norway the paleic surface reaches maximum elevations of >1500 m. Peaks rising above this level (e.g. Jotunheimen and Gaustatoppen in Telemark) are generally interpreted as residual or "old" mountains with a strong lithological control [*Peulvast*, 1985].

Although there is consensus on the events leading to the present geomorphology of Norway (i.e. peneplanation of the Caledonian mountain range followed by renewed uplift and incision) the timing of events and the age of the paleic surface remain controversial. *Gjessing* [1967] merely refers to the surface as "pre-glacial". Tentative dating of the paleic surface and the onset of uplift has been based mainly on a correlation with offshore unconformities. *Riis and Fjeldskaar* [1992] propose a Pliocene onset of uplift as an isostatic reaction to glacial erosion. On the other hand, *Torske* [1972] suggests a pre-Eocene age for the surface and "Tertiary" uplift, while *Doré* [1992] proposes a late Cretaceous age, based on a correlation of the paleic surface with the base Tertiary surface offshore. Finally, *Riis* [1995] suggests a multitude of ages for the paleic surface, including a Jurassic, Paleogene and Neogene phase derived from a correlation of morphological surfaces with offshore geology. Late Paleocene and early Eocene marine diatoms are encountered at elevations of ~300 m in Sweden [*Fenner*, 1988]. The morphology of the fjords in western Norway suggests that they were incised by glacial erosion into preexisting valleys cut into the paleic surface [*Nesje and Whillans*, 1994]. Therefore, uplift of the paleic surface seems to significantly predate glaciation and most probably started in the Late Oligocene [*Stuevold et al.*, 1992].

Apatite Fission Track Thermochronology

Sampling and Procedures

Samples for apatite fission track analysis were collected along two roughly E-W and NW-SE trending profiles and three elevation profiles (Figure 2). Samples comprise Precambrian as well as Caledonian metamorphic rocks, a Devonian sandstone, and a Triassic dike. Employed sample preparation and processing techniques are outlined by *Andriessen and Bos* [1986] and *Rohrman et al.* [1994]. Eleven samples were dated by the population method with an absolute age calculation; all other samples were dated by the external detector method using a Zeta calibration approach [*Hurford and Green*, 1983]. Age standards employed are Durango, Mt. Dromedary and Fish Canyon apatites, all constants and procedures are similar to those in *Rohrman et al.* [1994]. Errors were calculated using the standard approaches for the external detector [*Green*, 1981] and population [*Naeser et al.*, 1979] methods.

Results

Apatite fission track data are summarized in Table 1; ages are quoted at ± 1σ throughout. Three elevation profiles were sampled (see Figure 2 for locations). A profile at Eidfjord, at the edge of the Hardangervidda plateau where the paleic surface lies around 1000 m, samples an elevation interval from 0 to 1620 m. The second profile was collected at Jotunheimen, where the highest peaks of Norway occur, and ranges from 0 to 2465 m. At Gaustatoppen, a single peak rising ~800 m above the paleic surface in Telemark, a profile spanning an elevation from 480 to 1883 m, was collected. In addition, we reproduce a profile collected by *Andriessen* [1990] over a limited elevation range at Hunnedalen, in the southwest of the study area. Results are shown in Figure 3.

The Eidfjord profile was already the focus of a reconnaissance study by *Andriessen and Bos* [1986]. Additional data collected for this study show a strong correlation of AFT ages with elevation; ages vary from 98±8 Ma near sea level to 166±31 Ma at 1620 m. Mean track lengths decrease from >13 to <12 μm with decreasing elevation, while track length distributions become broader. The highest sample (EID3) has an anomalously low mean track length of 12.4 μm; however, only 28 tracks could be measured.

The Jotunheimen suite of samples encompasses the largest relief. AFT ages range from 106±12 Ma at sea level to 167±11 Ma at 2465 m. Although the age-elevation gradient is steeper than that at Eidfjord, the overall trend is the same. Track lengths decrease from a mean of 13.5 μm with a symmetrical narrow distribution (σ = 1.2 μm) at 2465 m to 11.6 μm and a standard deviation of 2.0 μm at sea level.

In contrast, the profile at Hunnedalen shows a very poor correlation of AFT age with elevation. Ages vary from 160 to 260 Ma, with mean track lengths varying between 13.4 and 14.3 μm and standard deviations between 1.0 and 1.8 μm [*Andriessen,* 1990].

The Gausta profile shows a weak age-elevation correlation with some scatter; ages vary from 191±14 Ma at the top to 172±16 Ma at 480 m. Mean track lengths range from 12.9 to 13.7 μm, with a mean around ~13.4 μm.

A plot of AFT age versus mean length, including data from *Rohrman et al.* [1994] and *Andriessen* [1990], is shown in Figure 4. There is a clear decrease in mean track length with age for the younger samples (<160 Ma), with a concurrent broadening of the standard deviation to ~2 μm. Highest mean track lengths are recorded by samples in the 170 to 220 Ma age range, with a slight decrease in mean track length for ages exceeding 220 Ma. The χ^2 probabilities (Table 1) follow this trend; samples with young AFT ages and low mean track lengths fail the χ^2 test more often than other samples.

The AFT age distributions do not show a relation with the Caledonian orogenic structure. Two samples of post-Caledonian rocks were collected: an alkaline dike with a K-Ar age of ~220 Ma [*Færseth et al.,* 1976] (sample 92-15) and a Devonian sandstone (sample 93-3). AFT ages from these samples are indistinguishable from those of surrounding Precambrian rocks at 184±20 Ma and 119±10 Ma, respectively. This confirms the pattern observed in the age-elevation and age-length plots, indicative of a temperature history dominated by cooling since the Triassic-Jurassic.

While there is no relationship between AFT ages and onshore geology, there is a strong correlation between AFT ages and mean elevation. Figure 5 shows the distribution of AFT isochrons from samples at an elevation of < 500 m, suggesting a domelike shape. The domal pattern is also revealed when AFT results are plotted in cross section (Figure 6). The areas of highest elevation in southwestern Norway are correlated with the lowest AFT ages at sea level, around 100 Ma in the inner fjords. Ages increase toward the peaks of the high mountains and toward the west coast (~160 Ma), as well as to the south and east (> 200 Ma). The pattern thus defines a large-scale structural dome with a half wavelength of approximately 200 km and a slight asymmetry, with a steeper age gradient on the northwestern than on the southeastern side.

Profile A has a NW-SE orientation; ages near sea level decrease from 153±26 Ma at Vestkappen (93-4) to 106±12 Ma at Jotunheimen (JOT 17) and increase again in the Oslo region and toward the Swedish border. Additional data from *Grønlie et al.* [1994] and *Stiberg* [1993], from the Trondheim and Kristiansund areas, respectively, show ages exceeding 200 Ma at sea level in the north. An E-W transect (profile B) shows a similar domal pattern. AFT ages are >180 Ma at the west coast (92-1, 92-14) and decrease in age in the direction of Eidfjord to around 100 Ma (EID16, EID17). Moving further to the east, the ages increase again in the Oslofjord area to >170 Ma [*Rohrman et al,* 1994] and reach values of 220 Ma in southern Sweden at elevations around 300 m [*Zeck et al.,* 1988]. Our easternmost sample in central Sweden (dal 15) gives an age of 285±35 Ma and a mean track length of 11.5 μm; it fails χ^2. This agrees with our results in Figure 4, which suggest a decrease in mean track length for ages >220 Ma. The profiles indicate that the half amplitude of the AFT age dome is about 2 km.

Interpretation

For interpretation of the AFT age-elevation patterns we employ the partial annealing zone (PAZ) concept [e.g., *Wagner,* 1979]. The PAZ is the temperature interval over which annealing rates increase from very slow (> 1 b.y. for total annealing) to almost instantaneous (i.e. < 1 m.y.). For apatite the PAZ lies between 60-120°C. The PAZ is not only dependent upon temperature but also on the timescale over which the temperature conditions prevail and the chemical composition of the apatites [*Green et al.,* 1986]. This implies that the PAZ shifts to higher temperatures for rapid cooling rates (>1°C/m.y.) and to lower temperatures for slow cooling rates (~0.1°C/m.y.). In terrains exhumed rapidly, a break in slope in the age-elevation plot locates the base of the fossil PAZ and dates the onset of exhumation [e.g., *Gleadow and Fitzgerald,* 1987].

AFT data from the Siljan deep drill hole in central Sweden [*Andriessen and Verschure,* 1988] indicate a temperature of 105°C at ~5 km for total annealing, indicative of heating times ≥100 m.y. The present-day geothermal gradient of ~20°C/km for the Siljan drill hole thus seems to be more or less stable since ~100 Ma, at least for the inland areas. Heat flow data for onshore southern Norway suggest a similar thermal structure [*Balling,* 1990].

Table 1. Fission Track Analytical Data for Apatites From Paleozoic and Precambrian Rocks From Southern Norway

Sample	Elevation, m	Number of Grains	ρ_s (N_s) x10^6 cm^{-2}		ρ_i (N_i) x10^6 cm^{-2}		ρ_d (N_d) x10^6 cm^{-2}		Age $\pm 1\sigma$, Ma	$P(\chi^2)$ or $\bar{s}$, %	Mean Track Length, µm	Stand. Deviation, µm	Number of Tracks
92-1	35	13	1.108	(239)	1.909	(206)	2.5509	(13584)	181±23	10	12.9±0.1	1.3	100
92-3	35	20	1.825	(857)	3.191	(749)	0.0258	(1494)	171±11	<<1	12.9±0.1	1.5	102
									160± 9				
92-4	525	13	3.763	(346)	7.679	(353)	2.5509	(13584)	153±17	0	11.3±0.1	1.5	100
									177±16				
92-5	990	20	0.687	(186)	1.279	(173)	0.0258	(1494)	161±18	50	13.0±0.2	1.3	60
92-6	640	20	0.710	(483)	1.567	(533)	0.0258	(1494)	136±10	25	12.4±0.1	1.4	100
92-9	1020	20	1.075	(432)	2.125	(427)	0.0258	(1494)	151±12	25	12.2±0.1	1.4	100
92-10	1020	20	2.000	(773)	4.451	(860)	0.0258	(1494)	135±9	50	12.8±0.1	1.2	100
92-14	30	20	2.302	(540)	3.556	(417)	2.5509	(13584)	202±21	2.5	13.4±0.1	1.3	100
									225±17				
92-15	0	17	2.937	(499)	4.913	(423)	2.5509	(13584)	184±20	5			
93-1	0	20	0.515	(414)	1.329	(534)	0.0272	(1574)	122±9	2.5			
									128±5				
93-3	0	20	0.680	(305)	1.798	(403)	0.0272	(1574)	119±10	50	12.5±0.2	1.5	71
93-4	100	4	0.388	(75)	0.797	(77)	0.0272	(1574)	153±26	98			
93-5	0	20	0.273	(241)	0.629	(278)	0.0272	(1574)	137±13	50	12.0±0.3	0.9	7
93-6	0	6	0.373	(72)	1.066	(103)	0.0272	(1574)	110±18	25			
H273*	300	50	1.449	(2272)	0.411	(774)	0.889†		185±21	0.09	11.7±0.1	1.5	100
MA759*	400	50	0.488	(765)	0.1409	(221)	0.889†		182±15	0.06			
MA510*	100	50	1.222	(1916)	0.2857	(448)	0.889†		224±17	0.06			
MA765*	150	50	0.555	(871)	0.132	(207)	0.889†		220±20	0.08			
MA281*	400	50	2.681	(1051)	0.605	(237)	0.889†		232±17	0.06			
S206*	700	50	3.023	(1185)	0.691	(271)	0.889†		229±13	0.05			
N472*	150	50	0.796	(1248)	0.223	(349)	0.889†		187±27	0.10			
dal15	500	15	1.177	(539)	1.254	(287)	0.0299	(1837)	285±35	2.5	11.5±0.2	1.6	100
									325±48				
							Eidfjord						
EID3*	1620	50	0.30	(264)	0.23	(205)	2.18†		166±31	0.09	12.4±0.3	1.4	28
EID5*	700	50	4.61	(1809)	4.44	(1740)	2.18†		134±8	0.04	12.1±0.1	1.4	100
EID11	1230	20	1.510	(750)	2.993	(743)	0.0258	(1494)	151±10	25	13.1±0.1	1.3	100
EID13	965	18	0.687	(514)	1.180	(441)	2.5509	(13584)	181±19	25	12.4±0.2	1.6	100
EID15	345	23	0.456	(451)	0.950	(470)	0.0258	(1494)	144±11	25	12.0±0.2	1.6	100
EID16	180	20	0.663	(382)	2.025	(583)	0.0258	(1494)	98±8	5	11.5±0.2	1.6	100
EID17	0	20	1.250	(488)	3.305	(645)	0.0258	(1494)	113±8	<<1	12.0±0.2	1.9	100
									117±5				
							Jotunheimen						
JOT1	2465	23	1.455	(745)	2.609	(668)	0.0258	(1494)	167±11	25	13.5±0.1	1.2	100
JOT3	2150	20	0.843	(420)	1.472	(367)	0.0258	(1494)	171±14	50	13.2±0.1	1.3	100
JOT5	1855	20	1.314	(640)	2.563	(615)	0.0258	(1494)	156±11	90	13.4±0.1	1.2	100
JOT9	1240	12	1.398	(370)	3.113	(412)	0.0258	(1494)	134±11	50			
JOT11	1430	20	2.767	(1283)	4.719	(1094)	0.0258	(1494)	175±10	25	12.6±0.1	1.2	100
JOT12	1010	19	1.883	(484)	4.188	(538)	0.0258	(1494)	135±10	2.5	12.5±0.1	1.4	100
									149±8				
JOT14	560	20	1.136	(406)	2.305	(412)	0.0258	(1494)	147±12	50			
JOT17	0	19	0.391	(151)	1.108	(214)	0.0258	(1494)	106±12	75	11.6±0.2	2.0	100
							Gausta						
GAU1	1845	14	2.397	(609)	3.778	(480)	0.0261	(1517)	191±14	75	13.6±0.4	1.4	12
GAU3	1670	10	3.980	(407)	4.968	(254)	2.5509	(13584)	248±29	10			
GAU5	1590	19	0.210	(105)	0.372	(93)	0.0261	(1517)	170±25	97.5	13.7±0.1	1.4	100
GAU7	1385	19	0.569	(275)	1.023	(247)	0.0258	(1494)	158±16	25	12.9±0.1	1.5	100
GAU9	1250	20	0.171	(63)	0.260	(48)	0.0261	(1517)	198±39	99.5	13.5±0.2	1.7	100
GAU11	980	7	0.3577	(51)	0.617	(44)	2.5509	(13584)	181±40	25	13.3±0.1	1.5	100
GAU12a	870	20	0.345	(132)	0.591	(113)	0.0261	(1517)	168±25	50	13.4±0.2	1.4	60
GAU15	480	18	3.462	(315)	5.827	(273)	0.0258	(1494)	172±16	10			

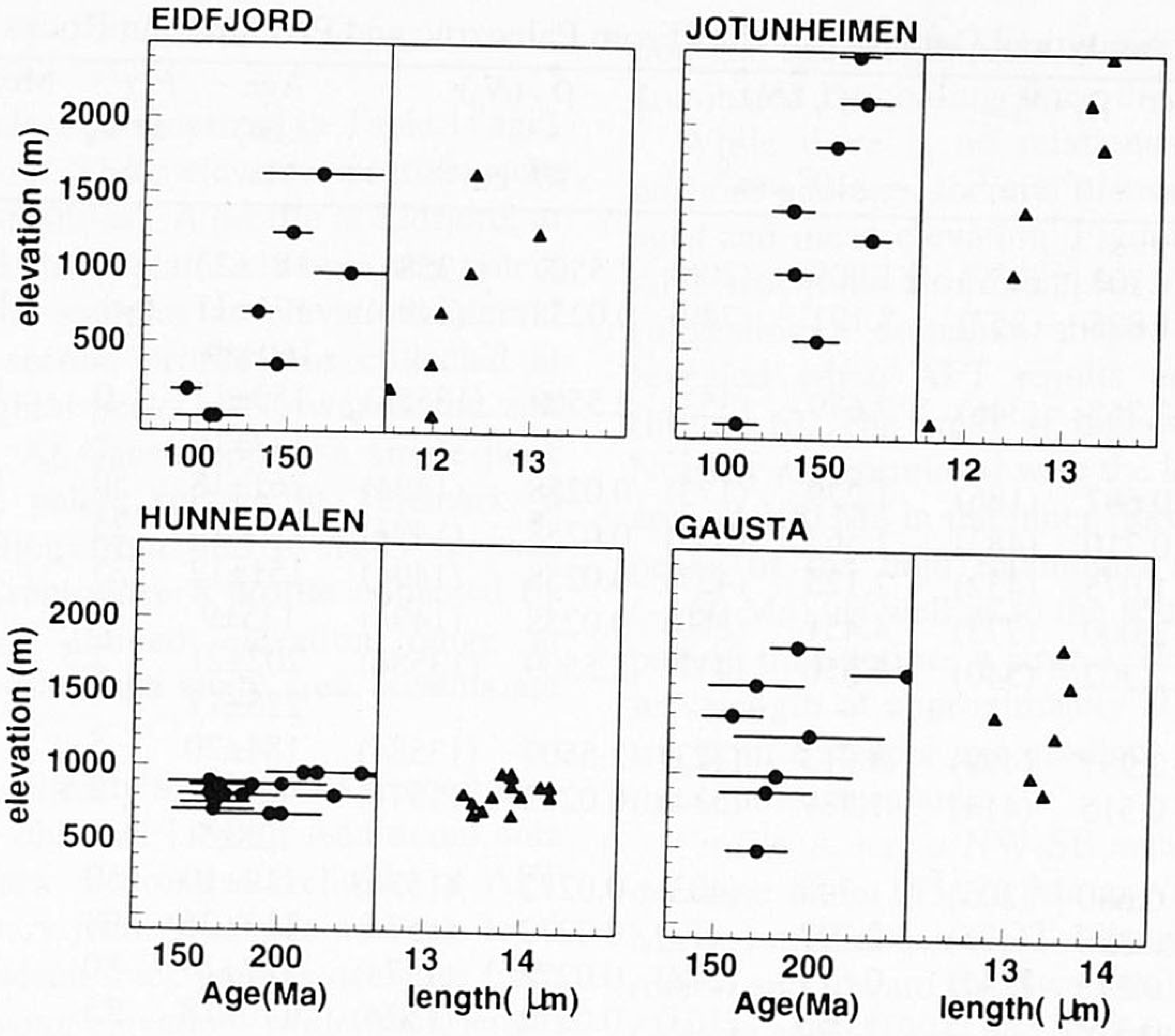

Figure 3. AFT age-elevation and mean length-elevation trends for four localities in southern Norway (see Figure 2 for locations). Hunnedalen data are from *Andriessen* [1990]; Eidfjord profile is partly from *Andriessen and Bos* [1986]. Note change in horizontal scale between upper and lower panels. Bars denote $\pm 1\sigma$ errors.

AFT age-elevation profiles in southern Norway (Figure 3) do not show breaks in slope. The Jotunheimen, Eidfjord, and Gausta profiles show a slow but consistent linear increase in age with increasing elevation, with the Gausta profile having somewhat older ages and longer mean track lengths. The Hunnedalen profile shows a more rapid increase with considerably more scatter. All profiles were collected in spatially restricted areas (highest and lowest samples are <20 km apart) in structurally homogeneous Precambrian basement. Thus the different elevation profiles seem to record different parts of a regional age-elevation trend. We interpret the Eidfjord and Jotunheimen suite of samples to originate from below a Jurassic PAZ, the Gausta samples from its base, and the Hunnedalen samples from within this PAZ (Figure 7). This would also explain the scatter in the Gausta and Hunnedalen profiles, as long residence times in the PAZ can cause differential annealing of grains resulting in scattered ages. Different age-elevation patterns across a study area have been used to suggest that the different profiles were separated by major faults [e.g., *Foster and Gleadow,* 1992]. However, no important post-Permian fault movements are known for onshore southern Norway; the entire area behaved as a single block from the Permian onward.

The interpreted Jurassic PAZ is consistent with the observed age-length trend; the constructed break in slope at ~160 Ma in Figure 7 agrees with the age-length peak in Figure 4. This cooling event, initiated at ~160 Ma, is coincident with the progradation of major deltas from the Norwegian mainland [*Doré,* 1991; *Steel,* 1993] and a major phase of rifting in the North Sea [*Ziegler,* 1990]. Mean track lengths in Figure 4 decrease for ages >220 Ma. This is more typical for the southern and eastern samples located around the Skagerrak, dating onset of exhumation for that part of the area [*Zeck et al.,* 1988; *Rohrman et al.,* 1994]. Evidence for erosion of this part of Fennoscandia is found in thick Triassic deposits associated with major faulting in the southern Skagerrak [e.g., *Jensen and Schmidt,* 1993]. Although AFT thermochronology strictly records cooling only, since the rapid cooling intervals coincide with periods of coarse clastic deposition with a Fennoscandian source offshore, we interpret them as erosional events. This implies that the Triassic-Jurassic was a major period of erosion in western Fennoscandia.

The youngest samples (~100 Ma) also have shortest mean lengths, broad track length distributions and low χ^2 probabilities (Figures 3 and 4 and Table 1), suggesting a long

Table 1. (continued)

Data presentation following *Hurford* [1990]. Abbreviations are ρ_s, spontaneous track density; ρ_i, induced track density (includes 0,5 geometry factor); N_s, N_i = number of tracks actually counted to determine the reported track density; $P(\chi^2)$, Chi-squared probability of having a single grain age distribution [*Galbraith,* 1981]. Samples are dated with the external detector method (except for the samples noted below), using the Zeta calibration approach; ζ=11760±425 for glass NBS963 and 124±7 for CN2 [*Rohrman et al.,* 1994] except for sample dal15, where ζ=10329±207 for glass NBS963 (PA). Ages for samples EID3 and EID5 are from *Andriessen and Bos* [1986]. For samples which fail theχ^2 test, the mean age is given together with the pooled age.

*Apatite age is determined by the population method with an absolute age calculation.

†Neutron fluence x10^{15} neutrons per square centimeter.

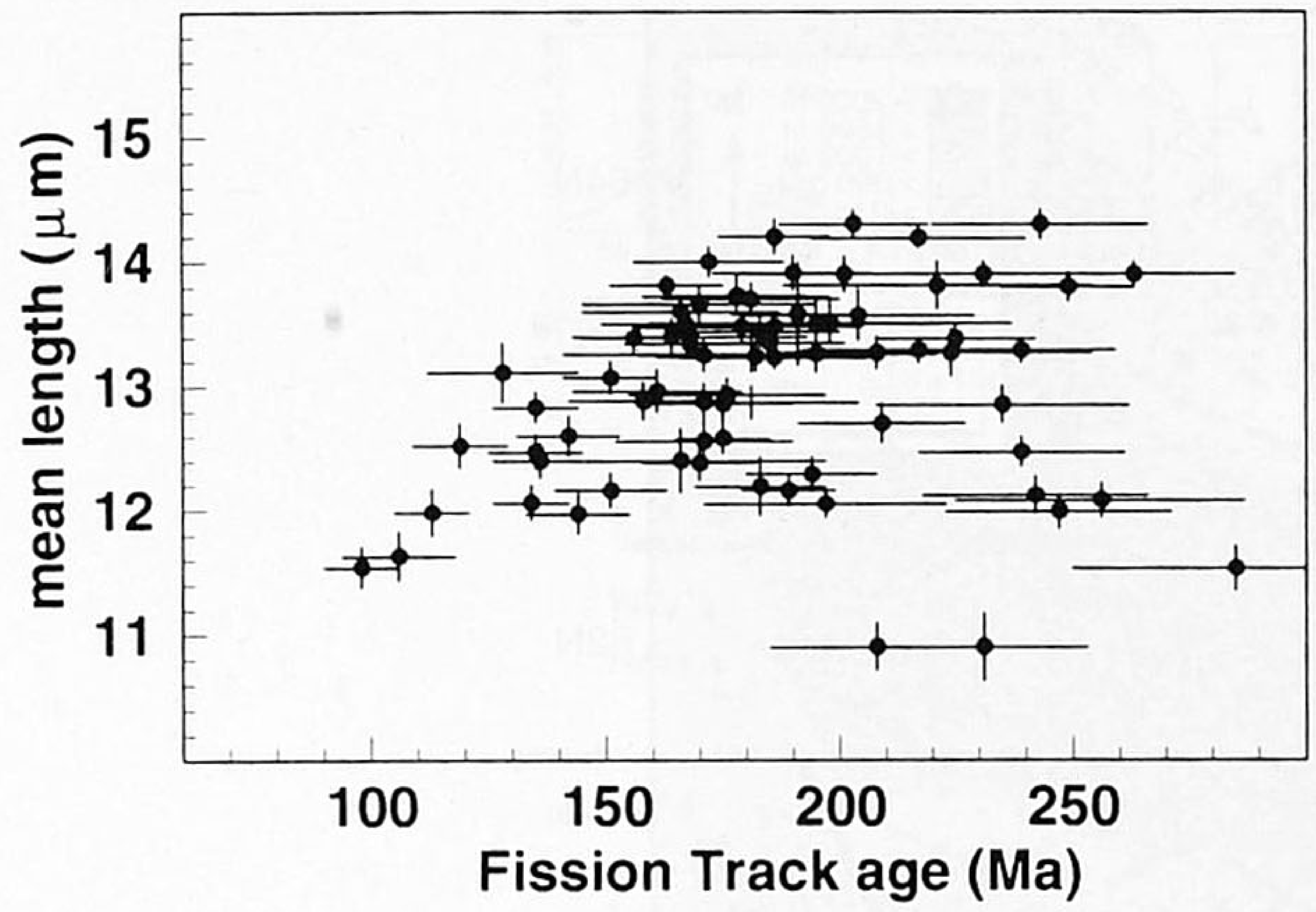

Figure 4. AFT age-mean length trend for southern Norway, including data from *Rohrman et al.* [1994], *Andriessen* [1990], and this study.

residence time in the PAZ before recent cooling. The pattern of isochrons (Figures 5 and 6) shows bending of isochrons as young as 100 Ma, indicating that final cooling was at least post-Cretaceous in age.

Thus, cooling seems to have taken place during two distinct time periods, one pre- and the other post-Cretaceous. We have performed forward and inverse modeling [e.g., *Lutz and Omar,* 1991] using the kinetic annealing model for F-apatites of *Crowley et al.* [1991] in order to further constrain the thermal history of the area. Chemical composition data from some of the apatites in this study suggest mainly F-rich varieties (Cl/(F+Cl)~0.0) [*Andriessen,* 1990], although there is probably considerable scatter in Cl content in our samples, since we collected many different lithologies. The Cl/(F+Cl) ratio is important for a quantitative interpretation of AFT data, since F-rich apatites anneal somewhat faster than Cl-rich grains [*Green et al.,* 1989]. We choose to employ the *Crowley et al.* [1991] annealing model because the (more popular) model of *Laslett et al.* [1987] seems to underestimate low-temperature and overestimate high-temperature annealing [e.g., *Corrigan,* 1993], thus possibly overemphasizing the importance of recent cooling. The *Crowley et al.* [1991] model exhibits an opposite behavior [*Corrigan,* 1993], thereby eliminating this model artifact.

Samples from the coastline and from the peaks of the high mountains are characterized by rapid Triassic-Jurassic cooling, with a rate of ~2-2.5°C/m.y. (Figures 8a and 8b). The low-temperature history in AFT inversions is not well constrained because of uncertainties in the annealing behavior for this temperature range; therefore we loosely interpret modeled temperatures ≤30-40°C as indicating that the samples reached near-surface conditions. This could have happened as early as Late Jurassic-Early Cretaceous for the above samples. In contrast, samples from sea level in the inner fjords indicate Neogene (< 30 Ma) final cooling from temperatures of 60-80°C, at a rate of 1-1.5°C/m.y. (Figure 8d). In between these periods of rapid cooling, lower rates (of the order of 0.5°C/m.y.) are inferred during the Cretaceous-Paleogene. A late acceleration of cooling rates, which is expected because of a possible increase in exhumation rate since the Pliocene and locally large glacial erosion in the fjords, is beyond the resolution of the data.

Most reconstructions of the paleic surface place it at an elevation of a few hundred meters near the shoreline [e.g., *Riis and Fjeldskaar,* 1992]. However, modeled thermal histories from coastline samples (e.g., Figure 8a) are more in accordance with samples from the mountain peaks (Figure 8b) than with those from the paleic surface at Hardangervidda (Figure 8c). The coastline sample shows rapid cooling to low ambient temperatures in the Early Jurassic, while the Hardangervidda sample was still at temperatures exceeding 120°C around that time. Cooling of the Hardangervidda sample commenced in the Late Jurassic, followed by slow cooling to near surface conditions during the Cretaceous and Paleogene, similar to the coastline sample. This suggests a Cretaceous or Paleogene age for the paleic surface, concordant with geomorphological interpretations [*Nesje and Whillans,* 1994]. With the present data we cannot determine whether the paleic surface was a continuous feature in the past [*Gjessing,* 1967] or actually consists of different surfaces which were not formerly continuous [*Peulvast,* 1985]. However, samples that are presently at sea level near the coastline seem to have come from the same structural level as those on the high mountain peaks, i.e. 1-1.5 km above the paleic surface'.

Figure 9 shows our preferred exhumation history, based on forward modelling of the "stacked" age-elevation plot (thick line in Figure 7) and inversion of length distributions for selected samples (Figure 8). Our model results suggest that late stage exhumation and related doming of AFT isochrons are predominantly Neogene events. The AFT isochrons represent pre-Neogene isotherms which were probably near horizontal planes. The large wavelength (~400 km) of the dome and denudation rates < 500 m/m.y. since the Neogene validate this assumption [*Stüwe et al.,* 1994]. Subsequent doming could be either the result of a post-Cretaceous thermal event which caused partial resetting of AFT ages, or of deformation by uplift and exhumation. We find little geological evidence for the first scenario; the present heat flow is low [*Balling,* 1990] and has probably been stable for ~100 Ma [*Andriessen and Verschure,* 1988]. We therefore propose that the domal pattern reflects differential uplift.

There is geological evidence offshore to suggest a distinct Neogene erosion event associated with uplift. Late Paleocene-early Eocene diatoms found on the Scandinavian mainland [*Fenner,* 1988] suggest that most of Fennoscandia was at or near sea level prior to the Neogene. Paleogene clastic wedges are restricted to the northwestern part of southern Norway and appear to be local in character [*Rundberg and Smalley,* 1989]. Although an onset of accelerating cooling rates from the Eocene on cannot be completely excluded from our thermal histories, the geological evidence strongly supports a Neogene cause. The structural basinward dip of pre-Neogene strata around southern Norway suggests Neogene domal uplift [*Doré,* 1992; *Stuevold et al.,* 1992], and the large Neogene wedge records associated erosion of the mainland. Uplift does not seem to have been accommodated by movement along the major fault zones. Detailed sedimentological studies of the Neogene wedge indicate that Neogene erosion was not an instantaneous event, and the timing of its onset may have differed along various parts of the wedge. Buildup of the wedge

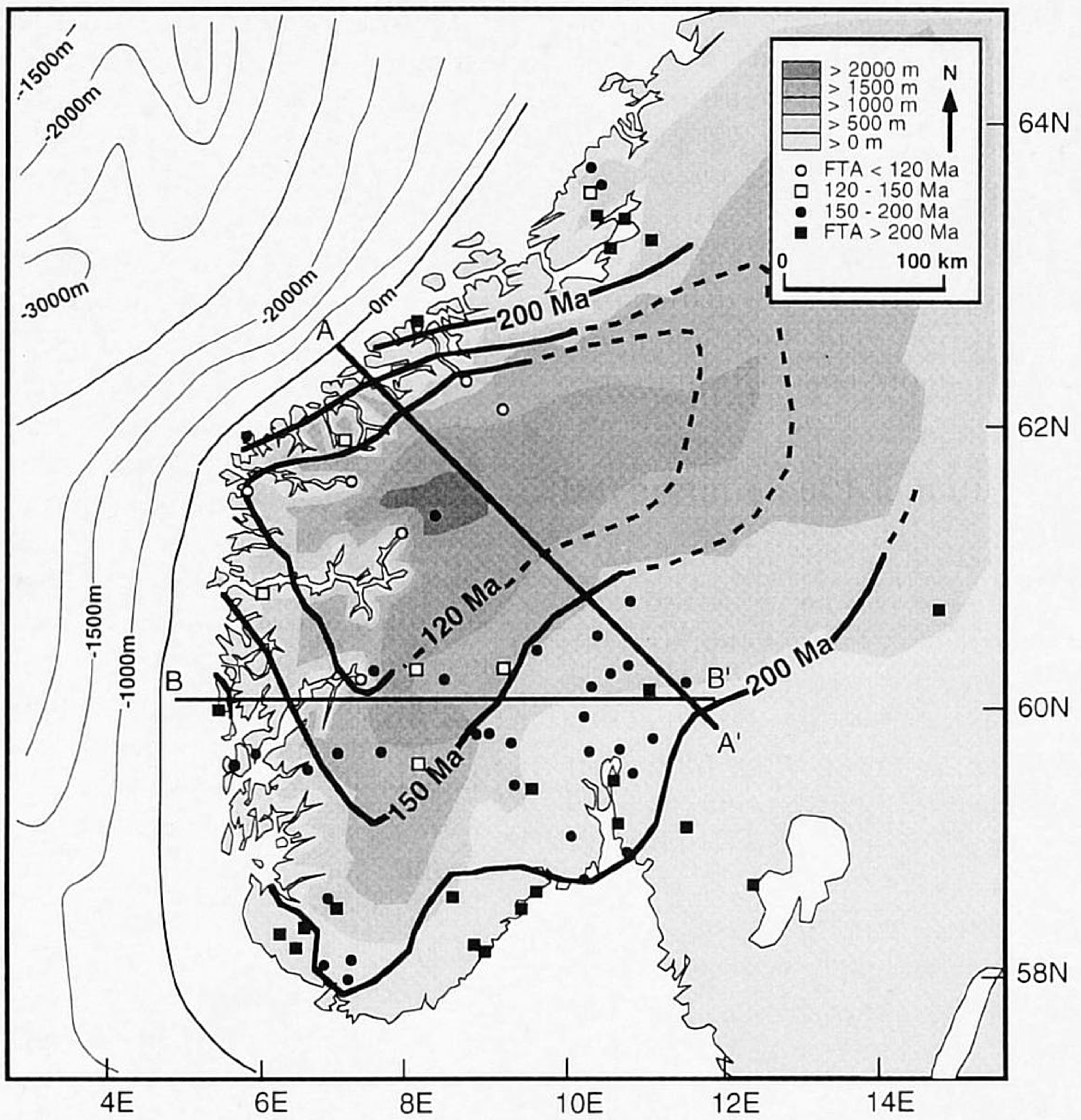

Figure 5. Regional variation of AFT ages plotted onto a map of mean topographic elevation. Fission-track samples are labeled according to age; isochrons of AFT ages are drawn for samples with an elevation < 500 m. Profiles A and B are depicted in Figure 6. Isolines offshore delineate isopachs of the Neogene wedge including the Oligocene (compiled and modified from *Vollset and Doré,* [1984], *Brekke and Riis* [1987], *Ziegler* [1990], and *Doré* [1992]).

started in the early Oligocene in the Norwegian-Danish basin [*Jensen and Schmidt,* 1993] and in the Late Oligocene in the Stord basin [*Ghazi,* 1992]; it accelerated in the Pliocene after a Miocene period of quiescence. Angular unconformities indicate that most of the erosion probably occurred in the Pliocene [e.g., *Ghazi,* 1992], coincident with increased basin subsidence [*Cloetingh et al.,* 1990].

Amount of Uplift and Erosion

We now consider quantifying the amount of tectonic uplift and exhumation from the inferred post-Permian thermal history. In order to estimate the amount of exhumation, we need to adopt a value for the geothermal gradient. Above, we have noted that the present-day geothermal gradient is approximately 20°C/km and that this has probably been stable for some time, at least further inland. However, the inferred thermal histories suggest that for example, samples from the top and base of the Jotunheimen profile, with a difference in elevation of 2.5 km, experienced a temperature difference of at least 70±20°C during the Late Jurassic-Early Cretaceous (Figures 8 and 9). This suggests that Mesozoic geothermal gradients could have been significantly higher than at present, of the order of 28±8°C/km. Although we cannot deduce a geothermal gradient for the Triassic-Jurassic we estimate it to be similar to the late Jurassic value (i.e., 30°C/km), leading to an estimate for Triassic-Jurassic erosion of 2.4±1.1 km. Neogene exhumation of samples from the inner fjords amounts to 2.0±0.5 km (i.e., 30-50°C cooling along a 20°C/km geotherm), decreasing radially outward to <0.5 km near the coastline. Cretaceous-Paleogene cooling can be interpreted as being related to relaxation of the geothermal gradient, combined with minor erosion resulting from ongoing deep weathering and slow removal of regolith.

To infer the amount of tectonic uplift from these numbers, we should know the amount of isostatic rebound as a response to erosion and the elevation prior to tectonic uplift [e.g., *Brown,* 1991; *van der Beek et al.,* 1994]. For the Triassic-Jurassic this is a difficult task; erosion seems to have been so widespread that isostatic rebound could have been substantial, whereas the elevation of Fennoscandia during this time interval is unknown. The deposition of thick sequences of continental deposits within the Triassic-Jurassic rifted grabens over long periods of time suggests that the elevation of the Laurasian continent could have been significant. The inferred exhumation is most probably the result of erosional base level lowering during rifting, combined with an unknown amount of tectonic rift flank uplift. For the Neogene history, we know that the area was close to sea level in the Paleogene [*Fenner,* 1988]. Using reasonable values for lithospheric strength (i.e., equivalent elastic thickness of the order of 15 to 60 km), tectonic uplift equals more than half of the amount of denudation [*van der Beek et al.,* 1994]. Therefore we can roughly estimate maximum Neogene tectonic uplift of southern Norway to have been of the order

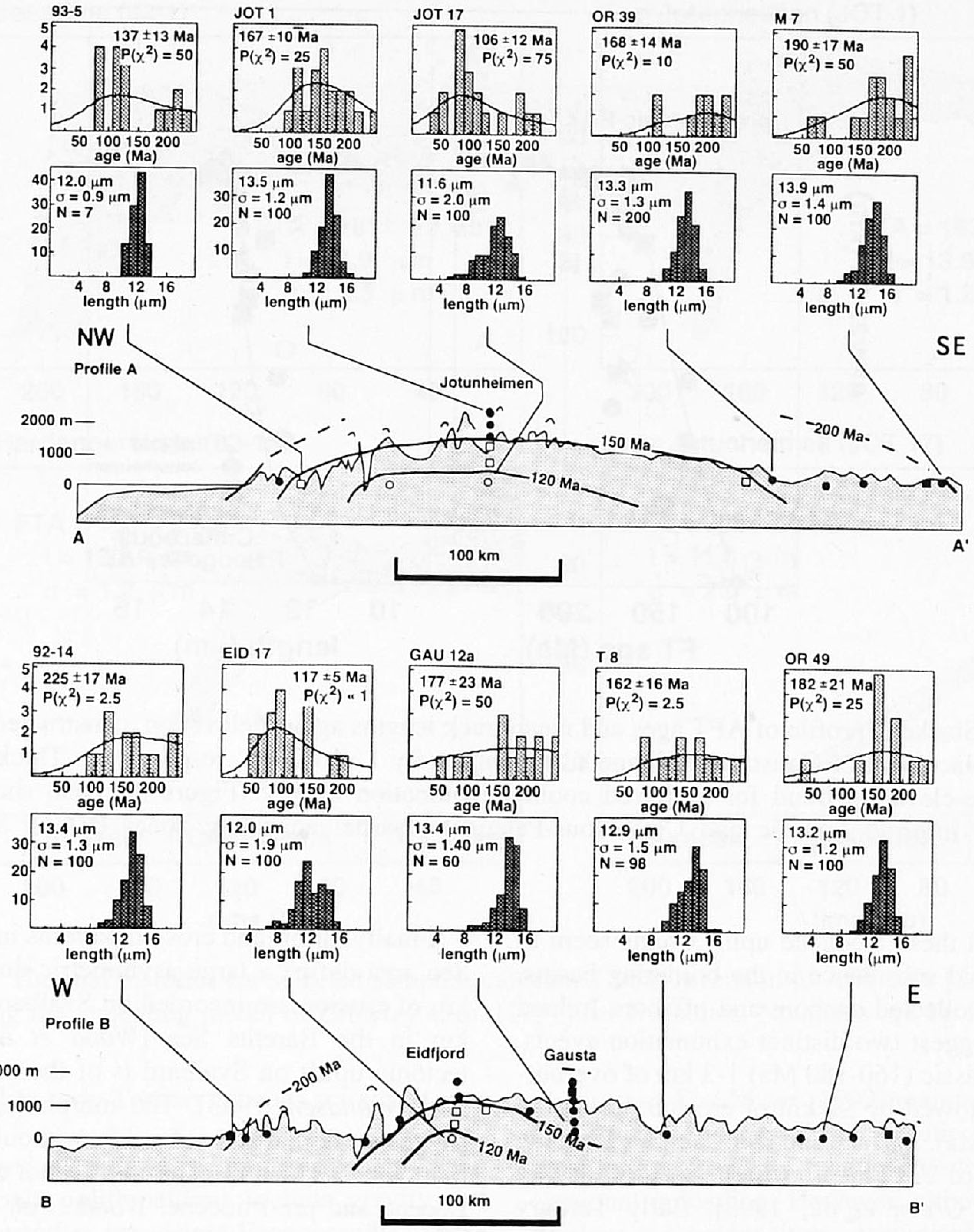

Figure 6. Selected AFT samples projected onto two profiles, A and B (location in Figure 5), showing domal deformation of AFT isochrons. Labeling of samples is the same as in Figure 5. Upper panels show AFT age histograms and probability curves; lower panels give length distribution histograms for selected samples. Topographic profiles are modified from *Torske* [1972]. Samples OR39, M7, T8, and OR49 are data from *Rohrman et al.* [1994].

of 1-1.5 km in the area of highest topography; the amount of uplift decreases radially outward to close to zero near the shoreline.

Uplift Mechanisms and Regional Implications

Our fission track results support a two-phase exhumation model for southern Norway. The southern and eastern parts of the study area, around the Skagerrak Graben, experienced a Triassic onset of exhumation [*Rohrman et al.*, 1994], and Jurassic erosion is dominant in western Norway. This Mesozoic phase was followed by slower exhumation during the Cretaceous-Paleogene, which resulted in a low elevation peneplanation of the area. Neogene domal uplift (from approximately 30 Ma onward) deformed this surface and, together with Plio-Pleistocene glacial erosion and isostatic rebound, created the present-day morphology of Norway. In the following we discuss the correlation with the evolution of the North Atlantic region, compare our results to other studies of uplift around the North Atlantic, and speculate on possible mechanisms creating Neogene domal uplift. In this discussion, we will use the term "tectonic uplift" only when there is evidence of a tectonic component; otherwise we loosely use the term "uplift" to denote both tectonic uplift and isostatic rebound.

Comparison With Other North Atlantic Margins

Tertiary uplift has been documented in other North Atlantic margins as well as in southern Norway. In a previous section we noted that Neogene tectonic uplift in western Fennoscandia forms three distinct structural and topographic domes, one in southwestern Norway, one in northern Sweden and Finnmark, and one in the Barents

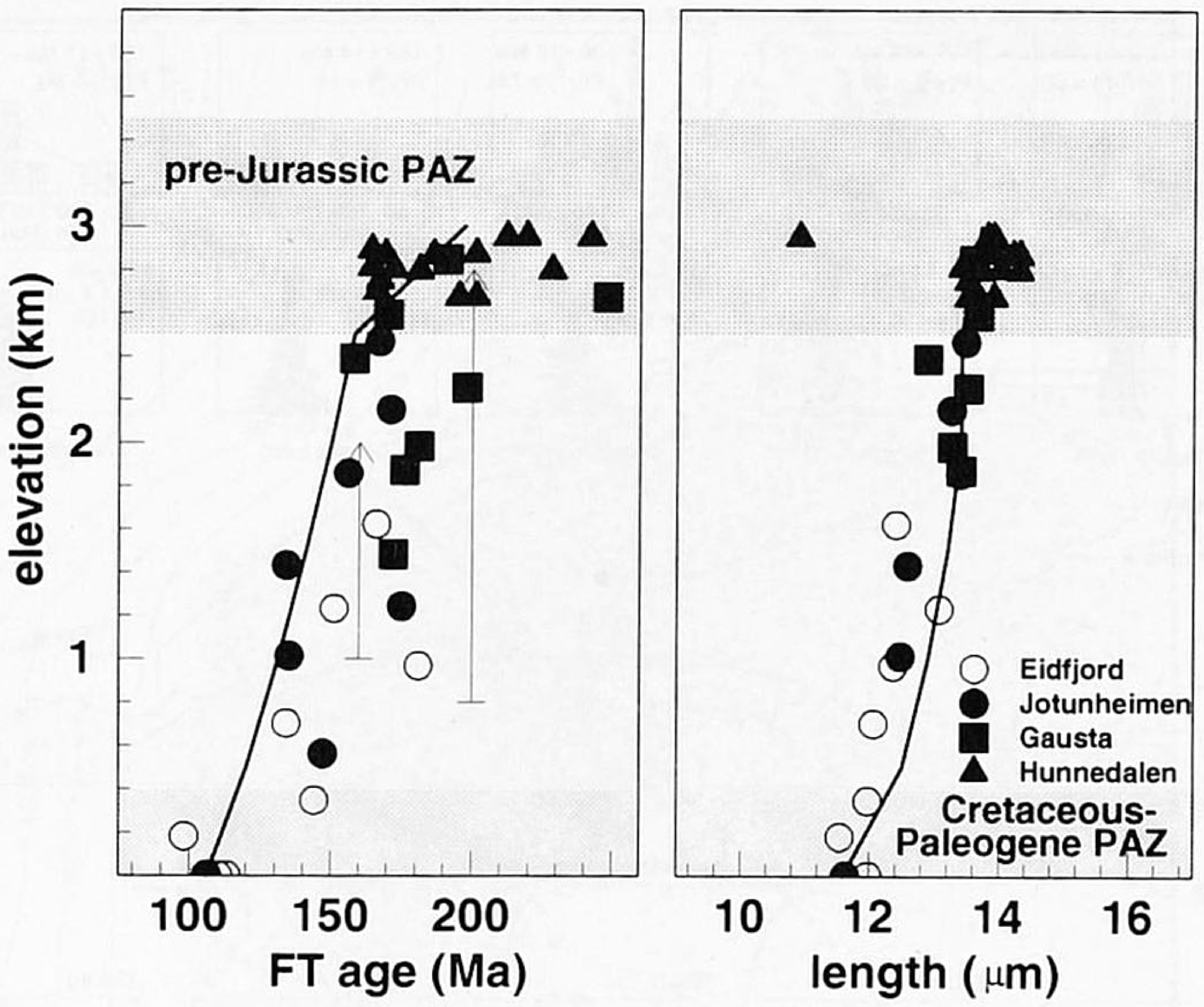

Figure 7. "Stacked" profile of AFT ages and mean track lengths against elevation, constructed by relative vertical displacement of Gausta and Hunnedalen samples by 1 and 2 km, respectively. Thick line shows modeled age-elevation trend for preferred cooling/exhumation history (Figure 9). Also shown are the positions of inferred Jurassic and Cretaceous-Paleogene partial annealing zones (PAZ). See text for discussion.

Sea/Svalbard area. All these Neogene uplift events seem to be associated with rapid subsidence in the bordering basins.

Fission track data collected onshore and offshore Ireland [*McCulloch,* 1993] suggest two distinct exhumation events. During the middle Jurassic (160-180 Ma) 1-3 km of overburden was removed, followed by ≤2 km of erosion during the early Tertiary (50-80 Ma). Surface and well samples from the United Kingdom record 2-3 km of erosion since 60-65 Ma [*Lewis et al.,* 1992; *Green et al.,* 1993]. Early Tertiary tectonic uplift and erosion of the British Isles are generally associated with contemporaneous, widespread igneous activity throughout the North Atlantic [*White and McKenzie,* 1989] and are possibly a result of magmatic underplating [*Brodie and White,* 1994]. However, *Green et al.* [1993] show, from modeling of AFT length distributions in well samples, that uplift and erosion are intermittent during the Tertiary and that possibly >50% of both took place after 30 Ma.

At the conjugate margin of mid-Norway, east Greenland, deeply eroded Paleo-Mesozoic basins and highly uplifted Paleocene flood basalts, emplaced near sea level, indicate post-eruptive uplift and erosion of the margin of the order of 1.5-2.5 km [*Larsen,* 1990; *Christiansen et al.,* 1992]. The fanning coastal dike complex of east Greenland, as well as the regional morphology, indicate a domal style of uplift [*Brooks,* 1985]. AFT data suggest periods of rapid exhumation around 200 Ma and 35 Ma [*Gleadow and Brooks,* 1979; *Hansen,* 1992]. The buildup of a large late Oligocene-recent offshore clastic wedge probably dates the initiation of uplift and erosion [*Larsen,* 1990]. Uplift of east Greenland is thus roughly synchronous with (or slightly precedes) Norwegian uplift but postdates volcanism and continental breakup by at least 15 to 25 m.y.

Finally, uplift and erosion patterns in the Svalbard/Barents Sea area define a large asymmetric dome. Approximately 3 km of erosion are recorded on Svalbard, decreasing to 1-1.5 km in the Barents Sea [*Wood et al.,* 1989]. Maximum tectonic uplift on Svalbard is of the order of 1 km [*Vågnes and Amundsen,* 1993]. The morphology of Svalbard again suggests a domal style of uplift, without reactivation of major fault zones. The timing of uplift is not well constrained: post-Eocene and pre-Pliocene. *Wood et al.* [1989] suggest that a major phase of tectonic uplift took place during the Oligocene (30-35 Ma). On the other hand, tectono-stratigraphic modeling by *Reemst et al.* [1994] suggests that the stratigraphy of the Barents Sea basins can be explained by a Miocene (15 Ma) sea level drop combined with flexural uplift from 5 Ma onward and Pleistocene glacial erosion.

Neogene Uplift Mechanisms

Several mechanisms have been suggested to explain the Neogene uplift of western Fennoscandia and other North Atlantic margins. Any model proposed should incorporate a number of critical geological and geophysical observations. Geomorphologic, structural and seismic data indicate that tectonic uplift of western Fennoscandia, the Barents Sea, and east Greenland was not associated with large vertical fault displacements. In the case of southern Norway, this study, together with geological constraints, supports a domal style of uplift. Also, the timing of uplift in these areas seems to be contemporaneous, being initiated in the Neogene (~30 Ma). This timing coincides with a major phase of plate reorganization in the North Atlantic [*Srivastava and Tapscott,* 1986; *Ziegler,* 1988], postdates initial breakup by 20-30 Ma, and significantly predates the onset of glaciation. Tectonic uplift and erosion of the British Isles were initiated earlier and

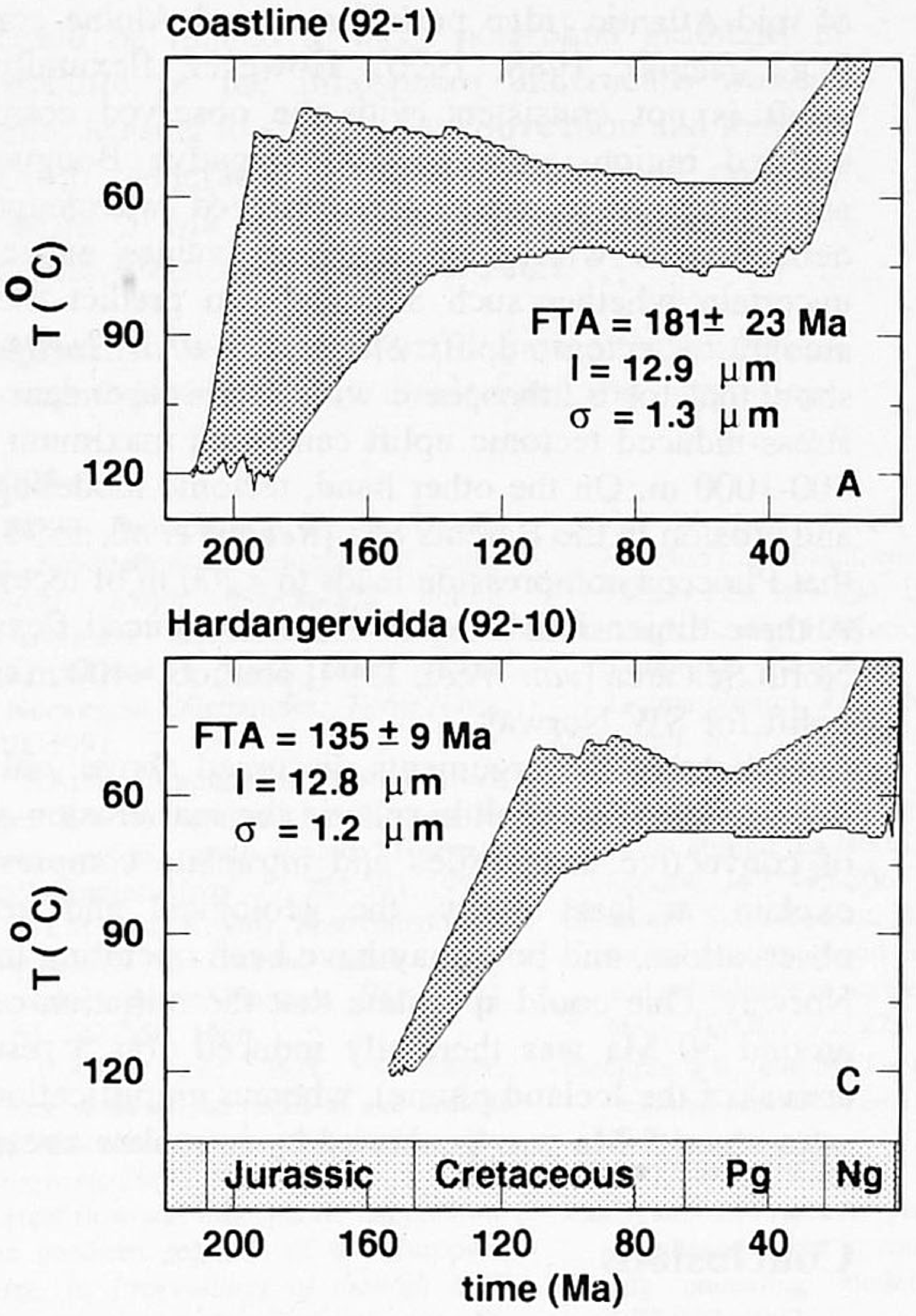

Figure 8. Thermal histories for selected samples, calculated from inversion of AFT data [*Lutz and Omar,* 1991] using the annealing model of *Crowley et al.* [1991] for F apatites. Notations are Pg Paleogene; Ng Neogene.

probably correspond to early Tertiary igneous activity [*Lewis et al.*, 1992].

Important geophysical data to take into account when explaining the tectonic uplift patterns include gravity and seismic tomography studies in western Fennoscandia. These studies indicate a marked feature of the two areas of domal uplift (Figure 1), both of them show strongly negative Bouguer gravity anomalies (down to -80 mGal in southwest Norway and -100 mGal in the north) [Sveriges Geologiska Undersökning, 1985] and strongly reduced lithospheric p and s wave velocities (down to -3%) [*Bannister et al.*, 1991]. The mass deficits that these data imply cannot be explained by differences in crustal structure and suggest an anomalous mantle structure and temperature underneath the domes [*Bannister et al.*, 1991].

Early models suggested that uplift of western Fennoscandia and other margins around the North Atlantic is associated with Paleocene breakup and plume activity [*Torske,* 1972; *White and McKenzie,* 1989]. Such models, however, obviously predict a timing for uplift of the margins around the Norwegian-Greenland Sea which is not consistent with available geomorphologic, sedimentologic, and thermochronologic data. Moreover, dynamic plume-generated uplift is transient and should reverse into subsidence 10-30 m.y. after breakup. Permanent uplift can be generated by magmatic underplating, but, in the case of the Norwegian margin, magmatic activity took place 300-400 km offshore [e.g., *Skogseid et al.,* 1992].

Riis and Fjeldskaar [1992] maintain that uplift of western Fennoscandia is a result of isostatic compensation to glacial erosion, amplified by mantle phase changes resulting from erosional unloading. However, although the major phase of erosion and redeposition, as indicated by sedimentological data, seems to have occurred from the Pliocene onward, this model cannot explain the initiation of uplift at ~30 Ma, long before the onset of glaciation. Moreover, the dynamics of mantle phase changes driving the tectonic uplift component in *Riis and Fjeldskaar*'s [1992] model are at present poorly understood.

A number of authors have proposed that Neogene uplift of western Fennoscandia is a result of thermal instability caused by large horizontal temperature gradients going from the Fennoscandian mainland to the Norwegian-Greenland Sea [e.g., *Theilen and Meissner,* 1979; *Peulvast,* 1985; *Vågnes and Amundsen,* 1993]. This would set up secondary convection in the sublithospheric mantle [*Fleitout and Yuen,* 1984; *Buck,* 1986], resulting in thermal erosion of the lithosphere underlying western Fennoscandia. Forward modeling indicates that secondary convection can generate ≤1 km of tectonic uplift for reasonable lithospheric strength values (characterized by equivalent elastic thicknesses of the order of 15-60 km) [*van der Beek et al.,* 1994]. Such an amount of tectonic uplift is small for synrift flank uplift but quite significant in a postrift setting such as this one. A model of thermal uplift is consistent with the observed gravity and seismic velocity lows under the uplifted regions in Norway.

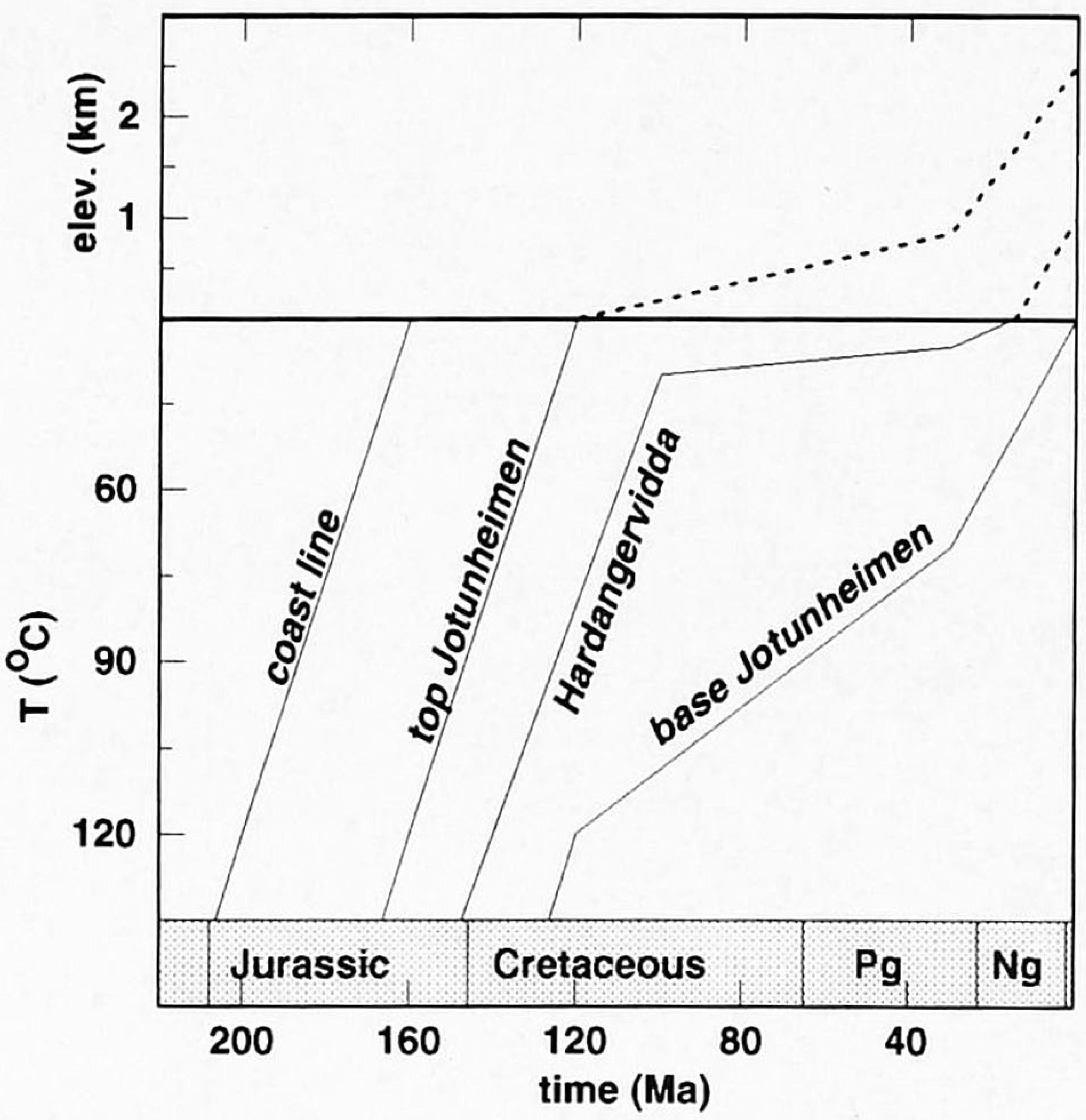

Figure 9. Preferred cooling and uplift trajectories for different groups of samples in the study area, based on forward modeling of the "stacked" age-elevation profile (thick line in Figure 7) and inverse modeling of selected samples (Figure 8). See text for discussion. Notations are Pg Paleogene; Ng Neogene.

Xenolith thermobarometry and the occurrence of hot springs on Svalbard suggest an abnormally thin lithosphere there [*Vågnes and Amundsen,* 1993]. In southern Norway, however, (sparse) heat-flow data do not indicate an increased geothermal gradient [*Balling,* 1990]. This model is also consistent with the inferred simultaneous uplift on both margins of the Norwegian-Greenland Sea, but why the uplift should be distributed into regional domes is not readily understood. Also, the timing of uplift with respect to breakup is not easily explained. Small-scale convection induced by rifting should generate synrift uplift [e.g., *Buck,* 1986]. However, it is possible that the convection pattern was not initiated by rifting and breakup itself but by the arrival of the Iceland plume in the region approximately 30-40 Ma ago [*Brooks,* 1985; *Lawver and Müller,* 1994]. Indeed, geoid and bathymetry data suggest that the mantle underlying the Norwegian-Greenland Sea is anomalously hot [*Cochran and Talwani,* 1978].

Finally, several authors have drawn attention to the synchronous timing of margin uplift and anomalous basin subsidence around the North Atlantic, suggesting that coupled uplift and subsidence is flexural in nature and induced by intraplate stress fluctuations [*Cloetingh et al.,* 1990, 1992; *Sales,* 1992]. Such a model explains the domal pattern of tectonic uplift and its synchroneity over a wide region. The onset of domal uplift in southern Norway is coincident with a late Oligocene plate reorganization; another reorganization at ~5 Ma could have resulted in accelerated uplift rates. The present-day stress field onland and offshore Fennoscandia is compressional and NW-SE oriented [*Müller et al.,* 1992], which is generally attributed to a combination of mid-Atlantic ridge push forces and Alpine compression [e.g., *Ziegler,* 1988; 1990]. However, flexurally induced uplift is not consistent with the observed correlation of uplifted regions with strongly negative Bouguer gravity anomalies. Also, while the observed wavelength of the deflection is within the range of values expected, it is uncertain whether such a model can predict the required amount of tectonic uplift. *Stephenson and Cloetingh* [1991] show that for a lithosphere with depth-dependent rheology, stress-induced tectonic uplift can reach maximum values of 500-1000 m. On the other hand, tectonic modeling of uplift and erosion in the Barents Sea [*Reemst et al.,* 1994] suggests that Pliocene compression leads to <200 m of tectonic uplift. A three dimensional model of stress-induced flexure in the North Sea area [*van Wees,* 1994] predicts <400 m of tectonic uplift for SW Norway.

In light of the arguments discussed above, only the last two models (i.e., sublithospheric thermal erosion as a result of convective instabilities and intraplate compression) can explain, at least partly, the geological and geophysical observations, and both may have been operating in southern Norway. One could speculate that the initiation of uplift at around 30 Ma was thermally induced (as a result of the arrival of the Iceland plume), whereas amplification of uplift rates since 5 Ma was generated by intraplate stresses.

Conclusions

Our AFT thermochronology study in southern Norway leads us to the following conclusions.

Regional AFT age patterns support a domal style of late stage postrift uplift in southern Norway. AFT ages show a strong correlation with topographic elevation patterns. Lowest ages (~100 Ma) are encountered at sea level in the inner fjords in the area of highest elevations, ages increase toward the peaks of the high mountains (to ~160 Ma) as well as radially away from this area (to > 200 Ma).

Modeling of AFT length distributions suggests two phases of exhumation. During Triassic-Jurassic times, approximately 1.3-3.5 km of overburden were removed, probably as a consequence of base level lowering and rift flank uplift. Triassic-Jurassic exhumation coincides with repeated rifting phases and the development of major clastic sequences in the North Sea area. This was followed by much slower exhumation rates during the Cretaceous-Paleogene. Geothermal gradients probably decreased from values near ~30°C/km in the Early Cretaceous to 20°C/km during the Late Cretaceous and Tertiary. Rapid exhumation caused by tectonic uplift started from ~30 Ma onward. Neogene tectonic uplift produced the domal pattern recognized in the topography and AFT data and was of the order of 1-1.5 km. Initiation of Neogene tectonic uplift significantly preceded Plio-Pleistocene glaciation of the area.

Uplift and exhumation in southern Norway are roughly synchronous with other margins of the Norwegian-Greenland Sea: northern Norway, Svalbard, the Barents Sea, and east Greenland. This places our results in a more regional framework. Rapid Neogene subsidence and margin uplift as encountered in southern Norway may be linked to similar processes around the North Atlantic region. The mechanism of uplift could be related to large horizontal gradients in thermal structure of the lithosphere underneath western Fennoscandia, leading to small-scale convection and thermal erosion. Uplift generated in this manner was possibly enhanced from 5 Ma onward by intraplate compression effects and Plio-Pleistocene glacial erosion.

Acknowledgments. We thank Bjørn T. Larsen (Norsk Hydro, Oslo) for support of this project, discussions, and suggestions. Tineke Vogel-Eissens and Lodewijk IJlst assisted in sample preparation and processing. This study is supported by the Netherlands Organization for Scientific Research NWO/GOA grant 750.530.25 to M.R. Irradiations were carried out at ECN, Petten, Netherlands. Jan Inge Faleide commented on an earlier version of the manuscript. Constructive reviews by Paul Fitzgerald and Roy Gabrielsen and comments by Tectonics editor Kevin Burke, are much appreciated. This is Netherlands Research School of Sedimentary Geology publication 941201.

References

Andersen, T.B., B. Jamtveit, J.F. Dewey, and E. Swensson, Subduction and eduction of continental crust: Major mechanisms during continent-continent collision and orogenic extensional collapse, a model based on the southern Norwegian Caledonides, *Terra Nova, 3,* 303-310, 1991.

Andriessen, P.A.M., Anomalous fission track apatite ages of the Precambrian basement in the Hunnedalen region, south-western Norway, *Nucl. Tracks Radiat. Meas., 17,* 285-291, 1990.

Andriessen, P.A.M., and A. Bos, Post-Caledonian thermal evolution and crustal uplift in the Eidfjord area, western Norway, *Nor. Geol. Tidsskr., 66,* 243-250, 1986.

Andriessen, P.A.M., and R.H. Verschure, Fission-track study of the rocks in and around the Siljan structure, Sweden, *Geol. Soc. Am. Abstr. Programs 20*(7), 1988.

Balling, N., Heat flow and lithospheric temperature along the northern segment of the European geotraverse, in *Proceedings of the 6th EGT Workshop,* edited by R. Freeman and St. Mueller, pp. 405-416, European Science Foundation, Strasbourg, France, 1990.

Bannister, S.C., B.O. Ruud, and E.S. Husebye, Tomographic estimates of sub-Moho seismic velocities in Fennoscandia and structural implications, *Tectonophysics, 189,* 37-53, 1991.

Bøe, R., and K. Bjerkli, Mesozoic sedimentary rocks in Edøyfjorden and Beitstadfjorden, central Norway: Implications for the structural history of the Møre-Trøndelag fault zone, *Marine Geology, 87,* 287-299, 1989.

Brekke, H., and F. Riis, Tectonics and basin evolution of the Norwegian shelf between 62°N and 72°N, *Nor. Geol. Tidsskr. 67,* 295-322, 1987.

Brodie, J., and N. White, Sedimentary basin inversion caused by igneous underplating: Northwest Europe continental shelf, *Geology, 22,* 147-150, 1994.

Brooks, C. K., Vertical crustal movements in the Tertiary of central east Greenland: A continental margin at a hotspot, in Morphotectonics of Rifted Continental Margins, edited by C. D. Ollier, *Z. Geomorphol. suppl., 54,* 101-117, 1985.

Brown, R.W., Backstacking apatite fission-track "stratigraphy": A method for resolving the erosional and isostatic components of tectonic uplift histories, *Geology, 19,* 74-77, 1991.

Brown, R.W., M.A. Summerfield, and A.J.W. Gleadow, Apatite fission track analysis: Its potential for the estimation of denudation rates and implications for models of long-term landscape development, in *Process Models and Theoretical Geomorphology,* edited by M.J. Kirkby, pp. 23-53, Wiley, 1994.

Buck, W.R., Small-scale convection induced by passive rifting: The cause for uplift of rift shoulders, *Earth Planet. Sci. Lett., 77,* 362-372, 1986.

Christiansen, F.G., H.C. Larsen, C. Marcussen, K. Hansen, H. Krabbe, S. Piasecki, L. Stemmerik, and W. Stuart Watt, Uplift study of the Jameson Land basin, east Greenland, *Nor. Geol. Tidsskr., 72,* 291-294, 1992.

Cloetingh, S., and H. Kooi, Intraplate stresses and dynamical aspects of rifted basins, *Tectonophysics, 215,* 167-185, 1992.

Cloetingh, S., F. Gradstein, H. Kooi, A.C. Grant and M. Kaminski, Plate reorganization: A cause of rapid late Neogene subsidence and sedimentation around the North Atlantic?, *J. Geol. Soc. London, 147,* 495-506, 1990.

Cloetingh, S., P. Reemst, H. Kooi, and S. Fanavoll, Intraplate stresses and the post-Cretaceous uplift and subsidence in northern Atlantic basins, *Nor. Geol. Tidsskr., 72,* 229-236, 1992.

Cochran, J.R., and M. Talwani, Gravity anomalies, regional elevation, and the deep structure of the North Atlantic, *J. Geophys. Res., 83,* 4907-4924, 1978.

Corrigan, J., Apatite fission-track analysis of Oligocene strata in south Texas, U.S.A.: Testing annealing models, *Chem. Geol. 104,* 227-249, 1993.

Crowley, K.D., M. Cameron, and R.L. Schaefer, Experimental studies of annealing of etched fission tracks in fluorapatite, *Geochim. Cosmochim. Acta, 55,* 1449-1465, 1991.

Doré, A.G., The structural foundation and evolution of Mesozoic seaways between Europe and the Arctic, *Paleogeogr. Paleoclimatol. Paleoecol., 87,* 441-492, 1991.

Doré, A.G., The base Tertiary surface of southern Norway and the northern North Sea, *Nor. Geol. Tidsskr., 72,* 259-265, 1992.

Færseth, R.B., R.M. McIntyre, and J. Naterstad, Mesozoic alkaline dikes in the Sunnhordland region, western Norway: Ages, geochemistry and regional significance, *Lithos, 9,* 332-345, 1976.

Fenner, J., Occurrences of pre-Quaternary diatoms in Scandinavia reconsidered, *Meyniana, 40,* 133-141, 1988.

Fleitout, L., and D. Yuen, Steady state, secondary convection beneath lithospheric plates with temperature- and pressure-dependent viscosity, *J. Geophys. Res., 89,* 9227-9244, 1984.

Foster, D.A., and A.J.W. Gleadow, The morphotectonic evolution of rift-margin mountains in central Kenya: Constraints from apatite fission-track thermochronology, *Earth Planet. Sci. Lett., 113,* 157-171, 1992.

Gabrielsen, R.H., Reactivation of faults on the Norwegian continental shelf and its implications for earthquake occurrence, in *Earthquakes at North-Atlantic Passive Margins: Neotectonics and Postglacial Rebound,* edited by S. Gregersen and P.W. Basham, pp. 67-90, Kluwer Academic, Norwell, Mass. 1989.

Gabrielsen, R.H., R.B. Færseth, R.J. Steel, S. Idil, and O.S. Klovjan, Architectural styles of basin fill in the northern Viking Graben, in *Tectonic Evolution of the North Sea Rifts,* edited by D.J. Blundell and A.D. Gibbs, pp. 158-179, Oxford University Press, New York, 1990.

Galbraith, R.F., On statistical models for fission track counts, *J. Int. Assoc. Math. Geol. 13,* 471-488, 1981.

Galloway, W.E., J.L. Garber, X. Liu, and B.J. Sloan, Sequence stratigraphic and depositional framework of the Cenozoic fill, central and northern North Sea, in *Petroleum Geology of Northwestern Europe: Proceedings of 4th Conference,* edited by J.R. Parker, pp. 299-315, Geological Society of London, 1993.

Ghazi, S.A., Cenozoic uplift in the Stord basin area and its consequences for exploration, *Nor. Geol. Tidsskr., 72,* 285-290, 1992.

Gjessing, J., Norway's paleic surface, *Norsk Geogr. Tidsskr., 21,* 69-132, 1967.

Gleadow, A.J.W., and C.K. Brooks, Fission track dating, thermal histories and tectonics of igneous intrusions in east Greenland, *Contrib. Mineral. Petrol. 71,* 45-60, 1979.

Gleadow, A.J.W. and P.G. Fitzgerald, Uplift history and structure of the Transantarctic Mountains: New evidence from fission track dating of basement apatite in the Dry Valleys area, southern Victoria Land, *Earth Planet. Sci. Lett., 82,* 1-14, 1987.

Green, P.F., A new look at statistics in fission track dating, *Nucl. Tracks Radiat. Meas., 5,* 77-86, 1981.

Green, P.F., I.R. Duddy, A.J.W. Gleadow, P.R. Tingate, and G.M. Laslett, Thermal annealing of fission tracks in apatite 1. A qualitative description, *Chem. Geol. 59,* 237-253, 1986.

Green, P.F., I.R. Duddy, G.M. Laslett, K.A. Hegarty, A.J.W. Gleadow and J.F. Lovering, Thermal annealing of fission tracks in apatite 4. Quantitative modelling techniques and extension to geological timescales, *Chem. Geol. 79,* 155-182, 1989.

Green, P.F., I.R. Duddy, R.J. Bray and C.L.E. Lewis, Elevated paleotemperatures prior to Early Tertiary cooling throughout the UK region: Implications for hydrocarbon generation, in *Petroleum Geology of NW Europe: Proceedings of 4th Conference,* edited by J.R. Parker, pp. 1067-1074, Geological Society of London, 1993.

Grønlie, A., C.W. Naeser, N.D. Naeser, J.G. Mitchell, B.A. Sturt, and D. Ineson, Fission-track and K-Ar dating of tectonic activity in a transect across the Møre-Trøndelag Fault Zone, central Norway, *Nor. Geol. Tidsskr., 74,* 24-34, 1994.

Hansen, K., Post-orogenic tectonic and thermal history of a rifted continental margin: The Scoresby Sund area, east Greenland, *Tectonophysics, 216,* 309-326, 1992.

Holtedahl, H., On the oblique uplift of some northern lands, *Norsk Geogr. Tidsskr., 14,* 132-139, 1953.

Hossack, J.R., and M.A. Cooper, Collision tecton ics in the Scandinavian Caledonides, in Collision Tectonics, edited by M.P. Coward and A.C. Ries, *Geol. Soc. Spec. Publ. London 19,* 287-304, 1986.

Hurford, A.J., International Union of Geological

Sciences subcommission on geochronology recommendation for the standardization of fission track dating calibration and data reporting, *Nucl. Tracks Radiat. Meas., 17,* 233-236, 1990.

Hurford, A.J., and P.F. Green, The zeta age calibration of fission-track dating, *Chem. Geol. 1,* Isotope geosci. sect., 285-317, 1983.

Jansen, E., and J. Sjøholm, Reconstruction of glaciation over the past 6 Myr from ice-borne deposits in the Norwegian Sea, *Nature, 349,* 600-603, 1991.

Jensen, L.N., and B.J. Schmidt, Neogene uplift and erosion in the northeastern North Sea; magnitude and consequences for hydrocarbon exploration in the Farsund Basin, in *Generation, Accumulation and Production of Europe's Hydrocarbons, European Association of Petroleum Geologists Special Publication, 3,* edited by A.M. Spencer, pp. 79-88, Florence, 1993.

Larsen, H.C., The east Greenland Shelf, in *The Geology of North America: The Arctic Ocean region,* edited by A. Grantz, L. Johnson and J.F. Sweeney, pp. 185-210, Geological Society of America, Boulder, Colo., 1990.

Laslett, G.M., P.F. Green, I.R. Duddy, and A.J.W. Gleadow, Thermal annealing of fission tracks in apatite 2. A quantitative analysis, *Chem. Geol. 65,* 1-13, 1987.

Lawver, L.A. and R.D. Müller, Iceland hotspot track, *Geology, 22,* 311-314, 1994.

Lewis, C.L.E., P.F. Green, A. Carter and A.J. Hurford, Elevated K/T palaeotemperatures throughout northwest England: Three kilometres of Tertiary erosion?, *Earth Planet. Sci. Lett., 112,* 131-145, 1992.

Lutz, T.M., and G.I. Omar, An inverse method of modeling thermal histories from apatite fission-track data, *Earth Planet. Sci. Lett., 104,* 181-195, 1991.

McCulloch, A.A., Apatite fission track results from Ireland and the Porcupine basin and their significance for the evolution of the North Atlantic, *Mar. Pet. Geol., 10,* 572-590, 1993.

Molnar, P., and P. England, Late Cenozoic uplift of mountain ranges and global climate change: Chicken or egg?, *Nature, 346,* 29-34, 1990.

Müller, B., M.L. Zoback, K. Fuchs, K. Mastin, S. Gregersen, N. Pavoni, O. Stephansson, and C. Ljungren, Regional patterns of tectonic stress in Europe, *J. Geophys. Res., 97,* 11,783-11,804, 1992.

Naeser, C.W., A.J.W. Gleadow, and G.A. Wagner, Standardization of fission-track data reports, *Nucl. Tracks Radiat. Meas., 3,* 133-136, 1979.

Nesje, A., and I.M. Whillans, Erosion of the Sognefjord, Norway, *Geomorphology, 9,* 33-45, 1994.

Neumann, E.-R., K.H. Olsen, W.S. Baldridge, and B. Sundvoll, The Oslo rift: A review, *Tectonophysics, 208,* 1-18, 1992.

Omar, G.I., M.S. Steckler, W.R. Buck and B.P. Kohn, Fission-track analysis of basement apatites at the western margin of the Gulf of Suez rift, Egypt: Evidence for synchroneity of uplift and subsidence, *Earth Planet. Sci. Lett., 94,* 316-328, 1989.

Peulvast, J.-P., Post-orogenic morphotectonic evolution of the Scandinavian Caledonides during the Mesozoic and Cenozoic, in *The Caledonide Orogen - Scandinavia and Related Areas,* edited by D.G. Gee and B.A. Sturt, pp. 979-995, John Wiley, New York, 1985.

Reemst, P.H.M., S. Cloetingh, and S. Fanavoll, Tectono-stratigraphic modelling of Cenozoic uplift and erosion in the SW Barents Sea, *Mar. Pet. Geol., 11,* 478-490, 1994.

Riis, F., Quantification of Cenozoic vertical move ments in Scandinavia by correlation of morphological surfaces with offshore data, *Global Planet. Change,* in press, 1995.

Riis, F. and W. Fjeldskaar, On the magnitude of the late Tertiary and Quaternary erosion and its significance for the uplift of Scandinavia and the Barents Sea, in *Structural and Tectonic Modelling and its Application to Petroleum Geology, NPF Special Publication, 1,* edited by R.M. Larsen, H. Brekke, B.T. Larsen and E. Talleraas, pp. 163-185, Elsevier, New York, 1992.

Roberts, D., and D.G. Gee, An introduction to the structure of the Scandinavian Caledonides, in *The Caledonide Orogen - Scandinavia and Related Areas,* edited by D.G. Gee and B.A. Sturt, pp. 55-61, John Wiley, New York, 1985.

Rohrman, M., P.A. van der Beek, and P.A.M. Andriessen, Syn-rift thermal structure and post-rift evolution of the Oslo Rift (SE Norway): New constraints from fission track thermo-chronology, *Earth Planet. Sci. Lett. 127,* 39-54, 1994.

Rundberg, Y., and P.C. Smalley, High-resolution dating of Cenozoic sediments from northern North Sea using $^{87}Sr/^{86}Sr$ stratigraphy, *AAPG Bull., 73,* 298-308, 1989.

Sales, J.K., Uplift and subsidence in northwestern Europe: Causes and influence on hydrocarbon entrapment, *Nor. Geol. Tidsskr., 72,* 253-258, 1992.

Skogseid, J., T. Pedersen, O. Eldholm and B.T. Larsen, Tectonism and magmatism during NE Atlantic continental break-up: the Vøring margin, in Magmatism and the Causes of Continental Break-up, edited by B. Storey, T. Alabaster and R.J. Pankhurst, 305-320, *Geol. Soc. Spec. Publ. London, 68,* 305-320, 1992.

Srivastava, S.P., and C.R. Tapscott, Plate kinematics of the North Atlantic, in *The Geology of North America: The Western North Atlantic Region,* edited by P.R. Vogt and B.E. Tucholke, pp. 379-401, Geological Society of America, Boulder, Colo., 1986.

Starmer, I., The Sveconorwegian orogeny in southern Norway, relative to deep crustal structures and events in the North Atlantic Proterozoic supercontinent, *Nor. Geol. Tiddskr., 73,* 109-132, 1993.

Steel, R.J., Triassic-Jurassic megasequence stratigraphy in the northern North Sea: Rift to post-rift evolution, in *Petroleum Geology of Northwestern Europe: Proceedings 4th Conference,* edited by J.R. Parker, pp. 299-315, Geological Society of London, 1993.

Stephenson, R.A., and S.A.P.L. Cloetingh, Some examples and mechanical aspects of continental lithospheric folding, *Tectonophysics, 188,* 27-37, 1991.

Stiberg, J.-P., Apatite fission track analysis from the Western Gneiss Region, preliminary results: Constraints to the Cenozoic uplift of the Norwegian passive margin (abstract), *Geonytt, 1,* 46, 1993.

Stuevold, L.M., J. Skogseid, and O. Eldholm, Post-Cretaceous uplift events on the Vøring continental margin, *Geology, 20,* 919-922, 1992.

Stüwe, K., L. White, and R. Brown, The influence of eroding topography on steady-state isotherms. Application to fission track analysis, *Earth Planet. Sci. Lett., 124,* 63-74, 1994.

Sveriges Geologiska Undersökning (SGU), Scandinavian Caledonides gravity anomaly map, in *The Caledonide Orogen - Scandinavia and Related Areas,* edited by D.G. Gee and B.A. Sturt, Wiley, Chichester, 1985.

Theilen, F. and R. Meissner, A comparison of crustal and upper mantle features in Fennoscandia and the Rhenish Shield, two areas of recent uplift, *Tectonophysics, 61,* 227-242, 1979.

Torske, T., Tertiary oblique uplift of western Fennoscandia; crustal warping in connection with rifting and break-up of the Laurasian continent, *Nor. Geol. Unders. Bull., 273,* 43-48, 1972.

Vågnes, E., and H.E.F. Amundsen, Late Cenozoic uplift and volcanism on Spitsbergen; caused by mantle convection?, *Geology, 21,* 251-254, 1993.

Van den haute, P., Apatite fission track dating of Precambrian intrusive rocks from southern Rogaland (south-western Norway), *Bull. Soc. Belge Géol., 86,* 97-110, 1977.

van der Beek, P.A., S. Cloetingh, and P.A.M. Andriessen, Mechanisms of extensional basin formation and vertical motions at rift flanks: Constraints from tectonic modelling and fission-track thermochronology, *Earth Planet. Sci. Lett., 121,* 417-433, 1994.

van Wees, J.D., 3D flexure and intraplate compression in the North Sea Basin: Implications for variations in necking depth and lithospheric rigidity, in Tectonic Modelling of Basin Deformation and Inversion Dynamics, Ph.D. thesis, pp. 133-152, Vrije Universiteit Amsterdam, 1994.

Verschure, R.H., Geochronological framework for the Late-Proterozoic evolution of the Baltic Shield in south Scandinavia, in *The Deep Proterozoic Crust in the North Atlantic Provinces,* edited by A.C. Tobi and J.L.R. Touret, pp. 381-410, *NATO ASI Ser. C,D,* Reidel, Norwell, Mass., 1985.

Vollset, J., and A.G. Doré, A revised Triassic and Jurassic lithostratigraphic nomenclature for the Norwegian North Sea, *Bull., 3,* pp. 1-50, Nor. Pet. Dir., Stavanger, 1984.

Wagner, G.A., Correction and interpretation of fission track ages, in *Lectures in Isotope Geology,* edited by E. Jäger and J.C. Hunziker, pp. 170-177, Springer-Verlag, New York, 1979.

White, R.S., and D.P. McKenzie, Magmatism at rift zones: The generation of volcanic continental margins and flood basalts, *J. Geophys. Res., 94,* 7685-7729, 1989.

Wood, R.J., S.P. Edrich, and I. Hutchison, Influence of North Atlantic tectonics on the large-scale uplift of the Stappen High and Loppa high, western Barents Shelf, in Extensional Tectonics and Stratigraphy of the North Atlantic Margins, edited by A.J. Tankard and H.R. Balkwill, *AAPG Mem. 46,* 559-566, 1989.

Zeck, H.P., P.A.M. Andriessen, K. Hansen, P.K. Jensen, and B.L. Rasmussen, Paleozoic paleo-cover of the southern part of the Fennoscandian Shield - Fission track constraints, *Tectonophysics, 149,* 61-66, 1988.

Ziegler, P.A., Evolution of the Arctic-North Atlantic and the Western Tethys, AAPG *Mem., 43,* 1988.

Ziegler, P.A., *Geological Atlas of Western and Central Europe,* Shell Internationale Petroleum Maatschappij, Den Haag, Netherlands, 1990.

P.A.M. Andriessen, S.A.P.L. Cloetingh, M. Rohrman and P.A. van der Beek, Faculty of Earth Sciences, Vrije Universiteit, De Boelelaan 1085, 1081 HV Amsterdam, the Netherlands. (e-mail: rohm@geo.vu.nl)

(Received August 8, 1994;
revised December 30, 1994;
accepted January 10, 1995.)